

γ CaMKII Shuttles Ca^{2+} /CaM to the Nucleus to Trigger CREB Phosphorylation and Gene Expression

Huan Ma,^{1,*} Rachel D. Groth,³ Samuel M. Cohen,¹ John F. Emery,¹ Boxing Li,¹ Esthelle Hoedt,² Guoan Zhang,² Thomas A. Neubert,² and Richard W. Tsien^{1,*}

¹Department of Neuroscience and Physiology, Neuroscience Institute, NYU Langone Medical Center, New York, NY 10016, USA

²Department of Biochemistry and Molecular Pharmacology and Skirball Institute, NYU Langone Medical Center, New York, NY 10016, USA

³Centers for Therapeutic Innovation, Pfizer, 1700 Owens Street, San Francisco, CA 94158, USA

*Correspondence: mahuan@gmail.com (H.M.), richard.tsien@nyumc.org (R.W.T.)

<http://dx.doi.org/10.1016/j.cell.2014.09.019>

SUMMARY

Activity-dependent CREB phosphorylation and gene expression are critical for long-term neuronal plasticity. Local signaling at Ca_v1 channels triggers these events, but how information is relayed onward to the nucleus remains unclear. Here, we report a mechanism that mediates long-distance communication within cells: a shuttle that transports Ca^{2+} /calmodulin from the surface membrane to the nucleus. We show that the shuttle protein is γ CaMKII, its phosphorylation at Thr287 by β CaMKII protects the Ca^{2+} /CaM signal, and CaN triggers its nuclear translocation. Both β CaMKII and CaN act in close proximity to Ca_v1 channels, supporting their dominance, whereas γ CaMKII operates as a carrier, not as a kinase. Upon arrival within the nucleus, Ca^{2+} /CaM activates CaMKK and its substrate CaMKIV, the CREB kinase. This mechanism resolves long-standing puzzles about CaM/CaMK-dependent signaling to the nucleus. The significance of the mechanism is emphasized by dysregulation of Ca_v1 , γ CaMKII, β CaMKII, and CaN in multiple neuropsychiatric disorders.

INTRODUCTION

Enduring neuronal plasticity requires communication between surface electrical events and nuclear gene expression (Deisseroth et al., 2003; Dolmetsch et al., 2001; Lonze and Ginty, 2002). Such “excitation-transcription (E-T) coupling” is exemplified by activity-dependent regulation of the transcription factor cAMP-response element binding protein (CREB), which is functionally important for learning and memory (Bartsch et al., 1998; Impey et al., 1996; Kandel, 2001; Yin et al., 1995). In mammalian neurons, this signaling is potentially initiated by Ca^{2+} influx through surface Ca_v1 (L-type) channels (Greenberg et al., 1986; Morgan and Curran, 1986; Murphy et al., 1991), but culminates micrometers away with activation of nuclear CREB (Deisseroth et al., 1996; Dolmetsch et al., 2001). Despite much study, basic questions persist about mechanisms that link neuronal activity to nuclear events.

Ca^{2+} binding to calmodulin (CaM) and consequent activation of Ca^{2+} /CaM-dependent protein kinases (Hudmon and Schulman, 2002; Kennedy, 2000) helps support E-T coupling (Wheeler et al., 2008, 2012; Wu et al., 2001). The CaM kinase family is most famous for α CaMKII, which contributes strongly to synaptic potentiation, learning, and memory (Giese et al., 1998; Lisman et al., 2002; Malinow et al., 1989; Silva et al., 1992; Wayman et al., 2008). Together with β CaMKII, α CaMKII participates in E-T coupling by gathering in signaling clusters within Ca_v1 channel nanodomains (Wheeler et al., 2008, 2012). Additional CaM kinases, CaMKIV and CaMKK, form a CaMK cascade within the nucleus (Means, 2000; Soderling, 1999). Neuronal activity and Ca^{2+} /CaM drive CaMKK to phosphorylate and activate nuclear CaMKIV, which phosphorylates CREB (Bito et al., 1996) and CREB-binding protein (CBP) (Impey et al., 2002), thus triggering gene expression. CaMK actions near the surface and within the nucleus are clearly distinct, but the link between these remains unclear.

This article features another CaMK family member, γ CaMKII, which is enriched in mammalian brain, but also expressed in heart, smooth muscle, liver, and immune cells (Bayer et al., 1999; Gangopadhyay et al., 2003; Tobimatsu and Fujisawa, 1989). Variations in its gene (CAMK2G) are associated with unreliable memory (de Quervain and Papassotiropoulos, 2006) and mental retardation (de Ligt et al., 2012). Here, we show that γ CaMKII provides a conduit between Ca^{2+} entry at the neuronal surface and nuclear transcriptional events. γ CaMKII operates as a vectorial transporter of sequestered Ca^{2+} /CaM, independent of any catalytic activity. Once delivered to the nucleus by γ CaMKII, Ca^{2+} /CaM triggers a highly cooperative activation of the nuclear CaMK cascade, rapid phosphorylation of CREB, and transcription of target genes. Our experiments demonstrate that the γ CaMKII shuttle is a long-sought mechanism to rapidly link voltage-gated opening of Ca_v1 Ca^{2+} channels to activity-dependent transcription.

RESULTS

Changes in Spatial Distribution of γ CaMKII upon Stimulation

Studies in cultured superior cervical ganglion (SCG) neurons indicated that E-T coupling is initiated in nanodomains just beneath the plasma membrane and involves clustering of CaMKII (α and β

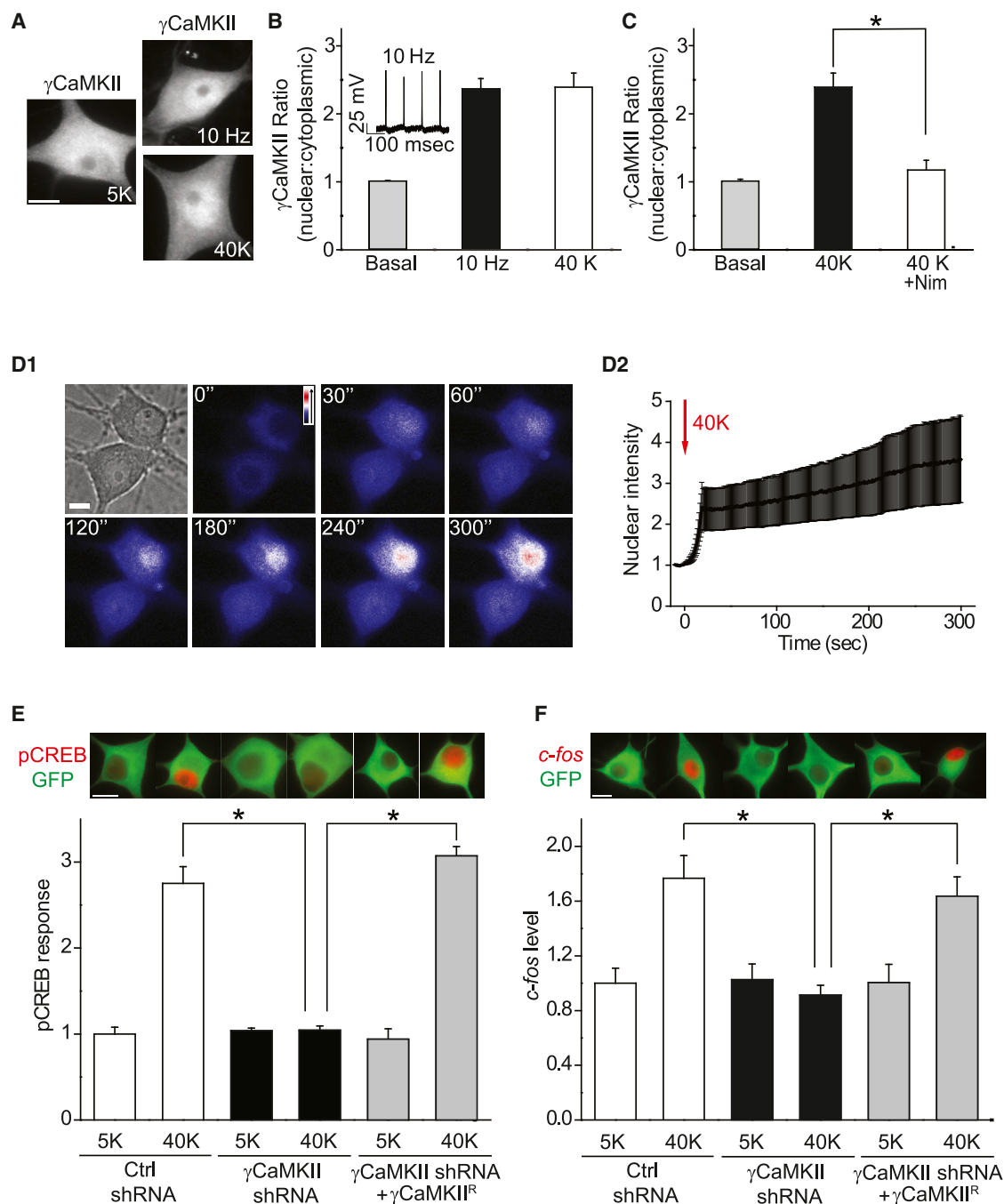


Figure 1. γ CaMKII Translocates to the Nucleus in an Activity-Dependent Manner and Is Critical for E-T Coupling

(A) SCG neurons were stimulated at 10 Hz for 60 s or exposed to 40 mM K^+ for 300 s and stained with a γ CaMKII antibody. Scale bar represents 10 μ m. (B) Increase in nuclear: cytoplasmic ratio of γ CaMKII intensity resulting from stimulation at 10 Hz for 60 s (solid bar) or from exposure to 40 mM K^+ for 300 s (open bar). Inset, recorded action potentials evoked by 10 Hz field stimulation. (C) γ CaMKII translocation triggered by 40 mM K^+ stimulation was abolished by the Ca_v1 -specific blocker Nim (10 μ M). (D1) mGFP- γ CaMKII translocation upon 40 mM K^+ stimulation. The bright field image indicates the cell shape, and other panels show epifluorescent images (union jack format) captured at indicated time points. (D2) Nuclear mGFP intensity, before and during 40 mM K^+ stimulation (onset, $t = 0$ s, $n = 4$). (E) SCG neurons expressing γ CaMKII shRNA or nonsilencing control shRNA were stimulated with 40 mM K^+ for 10 s and stained for pCREB (red). GFP (green) was used to confirm expression of plasmids. The pCREB response was prevented by γ CaMKII knockdown and rescued by overexpressing the shRNA-resistant γ CaMKII construct γ CaMKII^R (see Figures S1H–S1J for details).

(legend continued on next page)

isoforms) near Ca_v1 channels (Wheeler et al., 2008, 2012). These findings explained the reliance of E-T coupling on Ca_v1 channels but left open how a local aggregation of CaMKII at the surface causes signaling to the nucleus. Neither α CaMKII nor β CaMKII showed nuclear translocation following K^+ -depolarization, as in hippocampal neurons (Deisseroth et al., 1998); this also held for δ CaMKII (Figures S1A–S1C available online). However, the distribution of the γ CaMKII underwent an ~ 2.5 -fold increase in the nuclear: cytoplasmic intensity ratio upon depolarization with 40 mM K^+ , due to elevated nuclear intensity and diminished cytoplasmic intensity (Figures 1A and S1D). Similar changes were evoked by trains of spikes (10 Hz field stimulation) (Figures 1A and 1B). The depolarization-induced translocation of γ CaMKII to the nucleus was abolished by nimodipine (Nim) (Figure 1C), a Ca_v1 -specific channel blocker, indicating that Ca_v1 channels initiated the movement. To monitor the translocation in real time, we expressed a monomeric GFP-tagged γ CaMKII. The GFP- γ CaMKII fluorescence intensity consistently rose in the nucleus upon stimulation (Figures 1D1 and 1D2) and progressively decreased in the distal dendrites (Figures S1E and S1F), consistent with translocation of tagged γ CaMKII.

γ CaMKII Is Critical for Rapid CREB Phosphorylation and Gene Transcription

To find out whether γ CaMKII is required for E-T coupling, we studied the pCREB response following knockdown of γ CaMKII, performed with a lentivirus expressing short hairpin RNA (shRNA) specific to γ CaMKII. Stimulation by exposure to 40 mM K^+ for 10 s gave a robust but nonsaturating pCREB response (Figure S1G). Importantly, this pCREB response was strongly attenuated by γ CaMKII knockdown, but completely rescued by cotransfecting γ CaMKII cDNA that is resistant to γ CaMKII shRNA (indicated as γ CaMKII^R; Figures 1E and S1H–S1J). Furthermore, the sustained increase of CREB phosphorylation evoked by a 5 min depolarization was similarly abolished by γ CaMKII knockdown (Figure S1K), while the Ca^{2+} rise was not reduced (Figure S1L). Thus, regardless of whether stimuli were brief or prolonged, γ CaMKII contributed to Ca^{2+} -triggered CREB phosphorylation.

To examine effects of γ CaMKII on transcription, we tracked the CREB-dependent gene *c-fos* (Sheng et al., 1990). Depolarizing neurons with 40 K^+ for 5 min led to an ~ 2 -fold increase in *c-fos* levels (protein, Figure 1F; mRNA, Figure S1M). Strikingly, this increase in gene expression was prevented by γ CaMKII knockdown and rescued by γ CaMKII^R (Figures 1F and S1M). Thus γ CaMKII plays a critical role in supporting pCaMKII and CaM redistribution to the nucleus and in driving CREB phosphorylation and gene expression.

Redistribution of Phospho-CaMKII upon Stimulation

Like other CaMKs, γ CaMKII is regulated by phosphorylation at a particular threonine (α : Thr286; β , γ , and δ : Thr287) (Hudmon and Schulman, 2002; Kennedy, 2000). Finding that γ CaMKII is

critical for CREB phosphorylation led us to ask whether γ CaMKII translocates to the nucleus in a Thr287-phosphorylated state. We used an antibody specific for phospho-Thr286/287 CaMKII (pCaMKII) (not specific to any particular isoform) and compared the distributions of γ CaMKII and pCaMKII. Indeed, pCaMKII immunostaining revealed a clear nuclear redistribution in neurons subjected to field stimulation or 40 mM K^+ (Figures 2A, 2B, S2A, and S2B). Like γ CaMKII translocation, redistribution of pCaMKII in response to 40 mM K^+ was prevented by Nim (Figures S2C and S2D).

A strong correlation was found between depolarization-driven pCaMKII and γ CaMKII redistributions across a population of neurons (Figures 2C and S2E). A simple interpretation is that γ CaMKII translocated into the nucleus in a phospho-Thr287 form. We tested this by knocking down γ CaMKII with shRNA and found that the depolarization-dependent alteration in pCaMKII distribution was largely abolished (Figure 2D), indicating that pCaMKII redistribution was dominated by nuclear translocation of phosphorylated γ CaMKII.

CaM Redistribution Correlates with the Translocation of γ CaMKII

One consequence of CaMKII autophosphorylation at Thr286/287 is a $>1,000$ -fold increase in the affinity of CaMKII for Ca^{2+} /CaM (Meyer et al., 1992). Thus, phosphorylated CaMKII might sequester Ca^{2+} /CaM long after cytosolic Ca^{2+} had subsided (Deisseroth et al., 1998; Ma et al., 2012; Mermelstein et al., 2001). We next asked whether phospho- γ CaMKII and CaM might travel to the nucleus together, in line with the proposed role of CaM redistribution in E-T coupling (Deisseroth et al., 1998; Mermelstein et al., 2001). We costained neurons for CaM and γ CaMKII after 40 K^+ stimulation (Figure S2F). The ratios of nuclear: cytoplasmic intensities for CaM and γ CaMKII were highly correlated (Figure 2E). Similarly, correlation was found by directly comparing CaM translocation and pCaMKII redistribution (Figures S2G and S2H). Knockdown of γ CaMKII with shRNA eliminated the stimulation-dependent increase in nuclear: cytoplasmic ratio of CaM staining seen with control shRNA (Figure 2F). These results suggested that γ CaMKII translocated to the nucleus in a T287-phosphorylated form, accompanied by CaM. This would account for the reciprocal changes in nuclear and cytoplasmic levels of pCaMKII and CaM. Finally, the necessity of T287 phosphorylation was probed by an shRNA-resistant construct (γ CaMKII^R) encoding γ CaMKII with Thr287 mutated to Ala (γ CaMKII^R T287A). With endogenous γ CaMKII knocked down, “wild-type” γ CaMKII^R fully rescued CaM translocation (Figures 2G, left, S2I, and S2J). In contrast, γ CaMKII^R T287A was unable to rescue CaM translocation even though it translocated to the nucleus just as well as γ CaMKII^R (Figures 2G, right, S2I, and S2J). Taken together, these results suggest that γ CaMKII carries CaM into the nucleus because Thr287 phosphorylation engages CaM trapping (Hudmon and Schulman, 2002; Meyer et al., 1992).

(F) *c-fos* protein levels in SCG neurons transduced as in (E) and stimulated with 40 mM K^+ for 300 s, followed by 40 min incubation in normal culture medium to allow time for gene expression. γ CaMKII knockdown prevented the expression of *c-fos*, which was rescued by overexpressed γ CaMKII^R (see also Figure S1M). In all figures, the asterisk (*) denotes $p < 0.001$, as determined by Student's *t* test. Data are represented as mean \pm SEM. See also Figure S1.

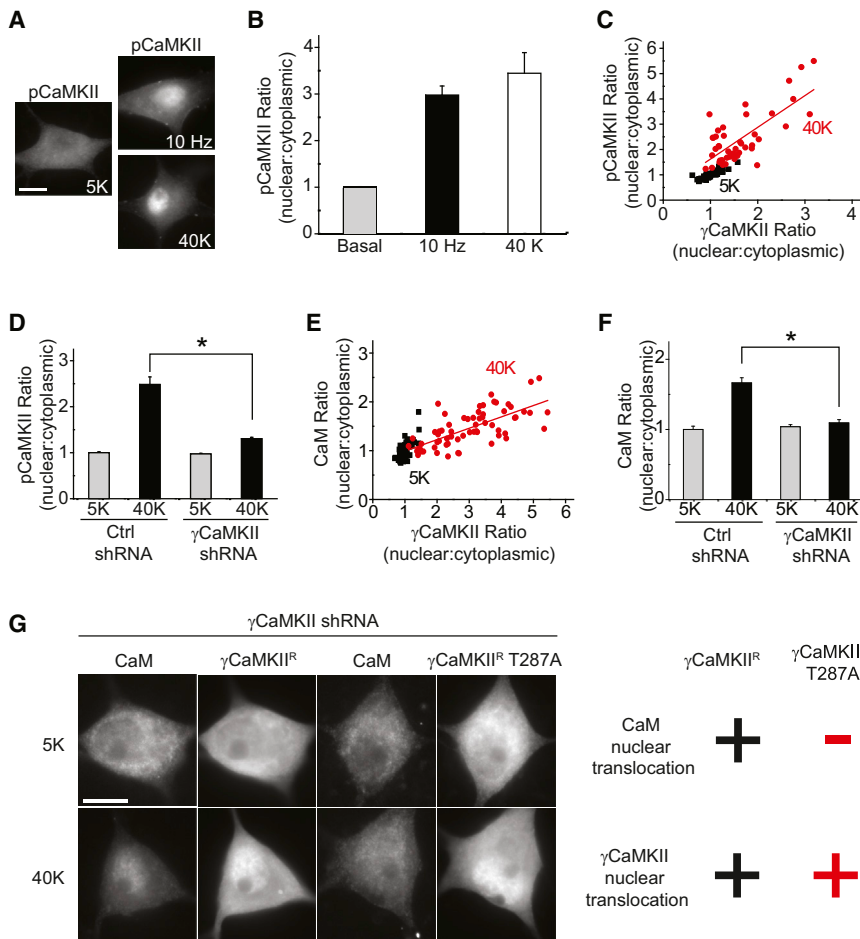


Figure 2. Activity-Dependent Nuclear pCaMKII Redistribution Is Driven by γ CaMKII/CaM Translocation

(A) SCG neurons were stimulated at 10 Hz for 60 s or with 40 mM K^+ for 300 s and stained for phospho-Thr286/287-CaMKII (pCaMKII). Scale bar represents 10 μ m.

(B) Pooled data for increase in ratio of nuclear:cytoplasmic pCaMKII intensities.

(C and E) Single-cell correlation of nuclear:cytoplasmic intensity ratio between pCaMKII and γ CaMKII ($R = 0.8$) or CaM and γ CaMKII ($R = 0.7$) in response to 40 mM K^+ , 300 s.

(D and F) SCG neurons expressing γ CaMKII shRNA or nonsilencing control shRNA stimulated as in (C). Increased nuclear:cytoplasmic ratios for pCaMKII and CaM were prevented by γ CaMKII knockdown. (G) With endogenous γ CaMKII knocked down, shRNA-resistant γ CaMKII^R or γ CaMKII^R T287A were overexpressed in SCG neurons. Upon stimulation as in (C), both γ CaMKII^R and γ CaMKII^R T287A translocated to the nucleus; however, only γ CaMKII^R, not γ CaMKII^R T287A, rescued CaM translocation. "+" and "-" indicate a significant or insignificant change respectively (see Figures S2I and S2J for details). See also Figure S2.

Cortical Neurons Also Display CaN-Regulated Translocation of γ CaMKII and CaM

We sought next to determine whether CaN-regulated γ CaMKII translocation exists in CNS neurons, focusing on pyramidal cells cultured from neocortex where γ CaMKII transcripts are prominent.

Indeed, K^+ -depolarization induced nuclear translocation of γ CaMKII and CaM in cortical pyramidal neurons, but not with Nim or CsA present (Figures 3D and 3E). To test whether CaN participates in CaMK-dependent excitation-pCREB coupling, we examined the pCREB response in cortical pyramidal neurons with a MEK1 inhibitor (PD98059) present to avoid engagement of the MAPK pathway (Dolmetsch et al., 2001; Wu et al., 2001). Importantly, depolarization-triggered CREB phosphorylation was inhibited by CaN inhibition with CsA (Figure 3F).

Capitalizing on the abundance of cultured cortical neurons, we isolated their nuclei and analyzed nuclear γ CaMKII levels by western blot. Consistent with immunostaining data, K^+ stimulation markedly elevated nuclear γ CaMKII, but not with Nim present (Figure 3G); cytoplasmic γ CaMKII was, if anything, slightly diminished (Figure S3F). Importantly, γ CaMKII knockdown also prevented CaM translocation and pCREB response (Figures 3H and 3I). Thus, CaM translocation and pCREB response in cortical neurons depends on both CaN and γ CaMKII, similar to what we found in SCG neurons.

Dephosphorylation of Ser334 by CaN Is Critical for γ CaMKII Translocation

To identify structural determinants of the translocation, we expressed HA-tagged γ_A CaMKII protein and probed its

γ CaMKII Needs to Be Dephosphorylated by CaN near the Cell Surface in order to Translocate to the Nucleus

How is the nuclear translocation of γ CaMKII regulated? Unlike γ CaMKII in the other tissues (Gangopadhyay et al., 2003; Takeuchi and Fujisawa, 1998), neuronal-specific γ CaMKII isoforms (γ_A , γ_A' , and γ_{AB}) each possess a nuclear localization signal (NLS) (Takeuchi et al., 2002). If the NLS confers nuclear localization, how might this be regulated? Notably, a serine (Ser334 in γ_A CaMKII) lies just C-terminal to the NLS in γ CaMKII (Figure S3A); phosphorylation of a similarly positioned serine inhibits nuclear localization in α_B CaMKII and δ_B CaMKII (Heist et al., 1998).

Seeking clues to such regulation, we first applied a broad range phosphatase inhibitor, PhosSTOP (PS), and found that PS inhibited γ CaMKII translocation and pCaMKII redistribution, without diminishing Ca^{2+} influx (Figure S3B–S3D). These results implied that some kind of phosphatase activity is required for γ CaMKII translocation. γ CaMKII translocation was unaffected by okadaic acid (OA) at 2 μ M, high enough to inhibit both PP1 and PP2A (Figure S3E). In contrast, γ CaMKII translocation was abolished by selective inhibition of calcineurin (CaN, also known as PP2B), using cyclosporin A (CsA) (Figure 3A) or FK506 (Figure S3E). CsA also prevented CaM translocation and the pCREB response (Figures 3B and 3C).

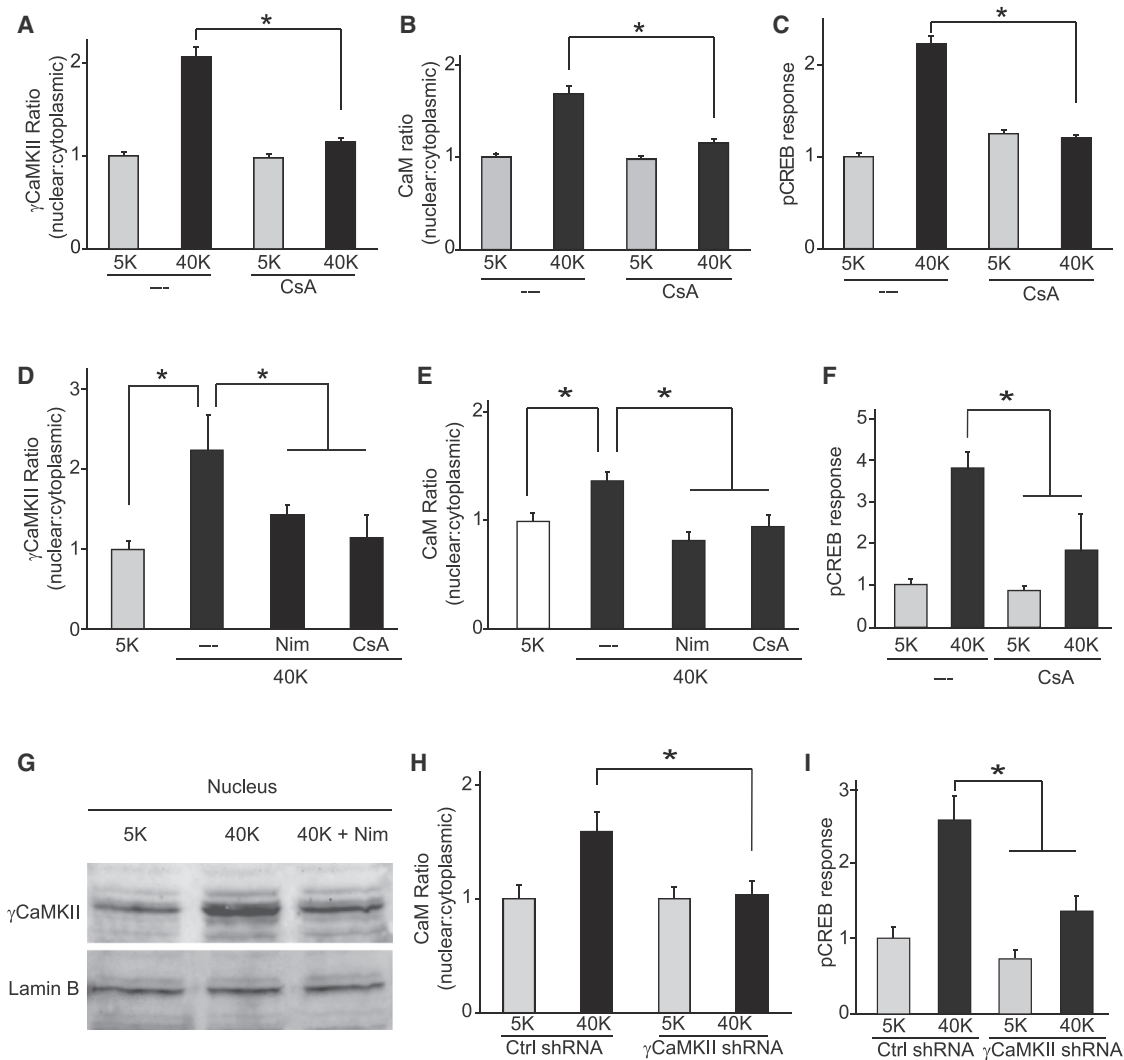


Figure 3. CaN Is Necessary for γ CaMKII/CaM Translocation and pCREB Response in SCG and Cortical Neurons

(A and B) SCG neurons stimulated with 40 mM K^+ for 300 s in absence or presence of calcineurin-specific inhibitor cyclosporin A (CsA, 50 nM). Translocation of both γ CaMKII (A) and CaM (B) prevented by exposure to CsA.

(C) pCREB response upon 40 mM K^+ stimulation for 10 s was prevented by CsA.

(D and E) Cultured cortical neurons were either mock-stimulated with 5 mM K^+ or stimulated with 40 mM K^+ for 60 s and stained for γ CaMKII or CaM (costaining with α CaMKII antibody to label excitatory neurons). Ca_v1 inhibitor Nim (10 μ M) or CaN inhibitor CsA (50 nM) prevented translocation of γ CaMKII and CaM.

(F) Cortical neurons treated as in (C), in additional presence of specific MEK inhibitor PD98059 (50 μ M), were stained for pCREB. pCREB response inhibited by CsA.

(G) Nuclei isolated from cultured cortical neurons and subjected to western blot analysis to probe for γ CaMKII. 40 mM K^+ stimulation of intact cells induced an increase of nuclear γ CaMKII that was prevented by Nim (N = 7). Lamin B is a nuclear marker.

(H) Cortical neurons transfected with either γ CaMKII shRNA or nonsilencing control shRNA, stimulated as in (D) and stained for CaM. γ CaMKII knockdown prevented CaM translocation.

(I) Cortical neurons expressing either γ CaMKII shRNA or a nonsilencing control shRNA. Stimulated pCREB response prevented by γ CaMKII knockdown.

See also Figure S3.

phosphorylation state with mass spectrometry (LC-MS/MS) (Figures 4A and 4B). The phosphorylation status of Ser334 and other candidate sites downstream was directly assessed. Ser334 was phosphorylated under basal conditions in HEK293 cells (Figures 4A and 4B), whereas the level of Ser334 phosphorylation was strongly decreased in vitro by exposure to purified CaN (Figure 4B, inset). This buttressed pharmacological evidence that

endogenous γ CaMKII is a target of CaN (Figure 3A) and supported Ser334 as a site of dephosphorylation.

To mimic the negative charge that phosphorylation confers, Ser334 of HA-tagged γ_A CaMKII was mutated to Glu ($\gamma_{A'}CaMKII$ S334E) and modified protein was localized with anti-HA antibody (Figure 4C). Like endogenous γ CaMKII, the HA-tagged “wild-type” γ_A CaMKII protein translocated to the nucleus upon

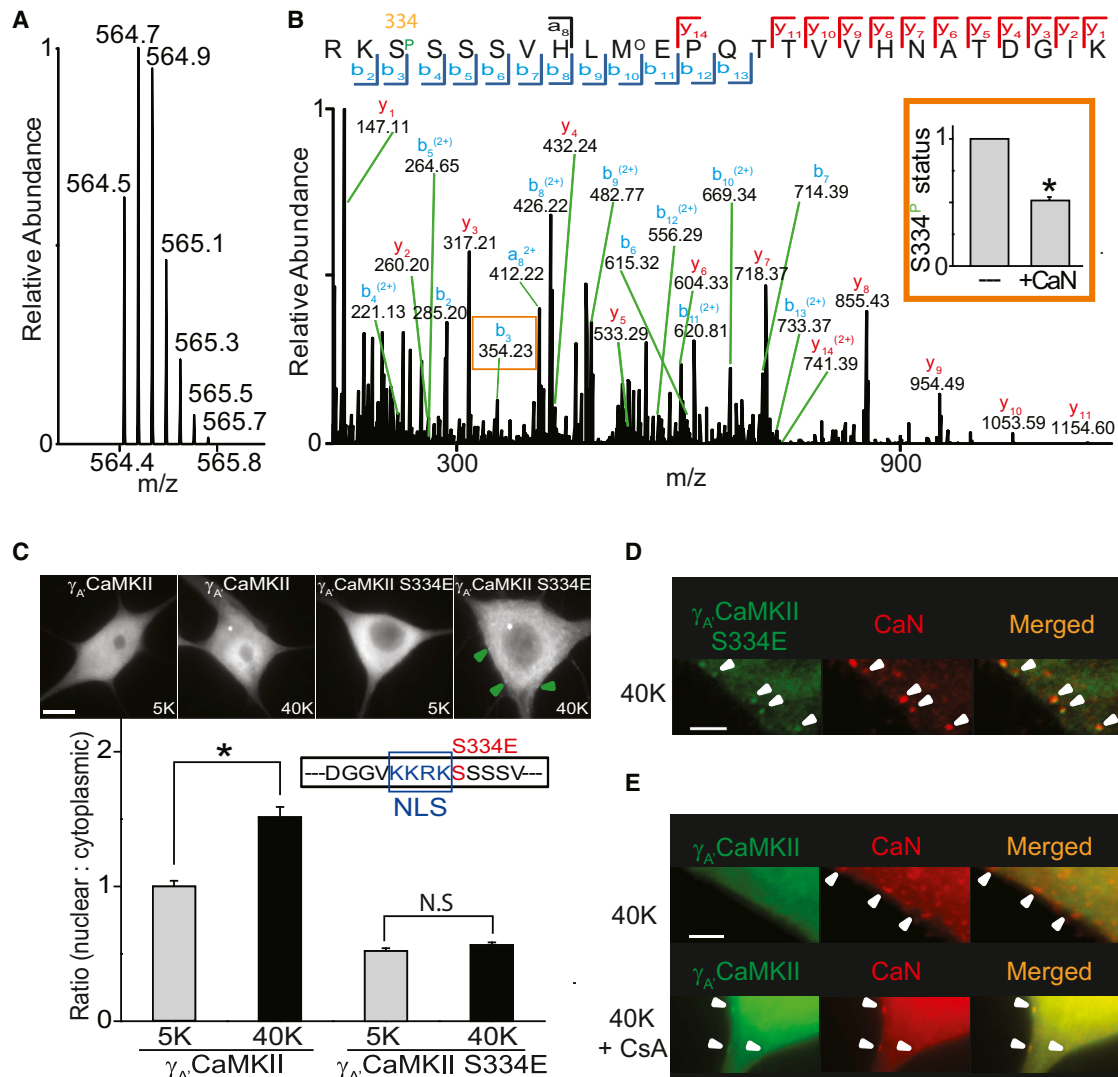


Figure 4. γ -CaMKII Is Dephosphorylated by CaN near the Cell Surface to Drive Nuclear Translocation

(A) Full scan mass spectrum of the quintuply charged ion (m/z 564.773) for the phosphopeptide RKS(Phospho)SSSVHLM(Oxidation)EPQTTVVHNATDGIK from γ_A -CaMKII.

(B) Tandem mass spectrometry (MS/MS) of the phosphopeptide RKS(Phospho)SSSVHLM(Oxidation)EPQTTVVHNATDGIK. MS/MS was performed on the quintuply charged ion (m/z 564.773) by using higher energy collision induced dissociation. The sequence of the peptide as well as the site of phosphorylation were confidently identified based on the matched b- and y-ion series indicated by the spectrum annotations. Note that all b-ions except the b2 ion correspond to fragments after neutral loss of phosphoric acid. The bar graph (insert) indicates that the phosphorylation status of S334 (marked by the orange square) was attenuated to $\sim 50\%$ of the control group after adding calcineurin and CaM for 30 min. N = 3 experiments, each done in triplicate.

(C) SCG neurons expressing γ_A -CaMKII or γ_A -CaMKII S334E stimulated with 40 mM K^+ for 300 s; γ_A but not γ_A -S334E translocated to the nucleus upon stimulation. Puncta of γ_A -CaMKII S334E formed on the cell surface upon stimulation marked by green arrows. Scale bar represents 10 μ m. Inset, position of S334E point mutation, just carboxyl to the nuclear localization sequence (NLS).

(D and E) Representative images of SCG neurons overexpressing γ_A -CaMKII S334E or γ_A -CaMKII, stimulated with 40 mM K^+ for 60 s. Arrowheads, sites where γ_A -CaMKII S334E puncta colocalize with CaN (D) or γ_A -CaMKII puncta colocalize with CaN in presence of CaN inhibitor CsA (lower panel) (E). No γ_A -CaMKII puncta formed without CaN inhibitor (upper panel) (E). Scale bar represents 5 μ m.

See also Figure S4.

40 mM K^+ stimulation (Figures 4C, left, and S4A), an event prevented by Nim, CsA or FK506 (Figure S4B). In contrast, the phosphomimetic γ_A -CaMKII S334E protein was mostly cytoplasmic under basal conditions and failed to undergo translocation upon stimulation (Figure 4C, right). Thus, dephosphorylation of

Ser334 of γ -CaMKII appears necessary for its nuclear translocation.

While failing to translocate to the nucleus, γ_A -CaMKII S334E nonetheless underwent redistribution, forming puncta near the surface membrane upon depolarization (Figure 4D). Such puncta

were not seen with γ_A CaMKII itself (Figure 4E, upper row) unless CaN was inhibited with CsA (Figure 4E, lower row). Evidently, inhibition of dephosphorylation, by phosphomimetic mutation or CaN inhibition, creates a biochemical bottleneck, causing γ_A CaMKII to pile up. The puncta mark sites where CaN-mediated dephosphorylation would normally initiate translocation to the nucleus. Indeed, puncta of γ_A CaMKII S334E coincided with puncta of CaN (Figure 4D, merged image). Similar colocalization was seen in multiple planes of focus (Figure S4C). γ_A CaMKII puncta also colocalized with CaN when CaN was inhibited with CsA (Figure 4E, bottom row). CaN puncta appeared no different when phosphatase activity was not inhibited (Figure 4E, top row). Without an imposed bottleneck, the lack of γ_A CaMKII puncta can be attributed to prompt CaN-triggered translocation to the nucleus.

γ CaMKII Travels to a Signaling Checkpoint in a CaM-Bound, but Not a Thr287-Phosphorylated, Form

We next focused on how γ CaMKII is recruited to these signaling checkpoints. The puncta formed by γ_A CaMKII S334E provided an assay of biochemical steps preceding its arrival at the checkpoint. Consistent with previous reports (Shen and Meyer, 1999), CaM binding to γ CaMKII was necessary to enable its recruitment to surface sites (see Figures S4D–S4I and legends for details). At what subsequent stage is γ CaMKII phosphorylated for sake of CaM trapping? A γ_A CaMKII construct with a phosphomimetic T287E mutation remained dispersed within the cytosol after stimulation (Figures S4J1 and S4J3). Similarly, a doubly altered γ_A CaMKII T287E, S334E construct failed to form puncta upon stimulation (Figures S4J2 and S4J4). Evidently, γ CaMKII cannot be mobilized from the cytosol and targeted to the cell surface when Thr287 is fully phosphorylated (Hudmon et al., 2005; Shen and Meyer, 1999). Thus, it is CaM-bound, but not fully Thr287-phosphorylated γ CaMKII that is recruited to the Ca_v1 checkpoints (Figure S4M). Such phosphorylation likely occurs before translocation to the nucleus because expression of the nuclear translocation-defective γ_A CaMKII S334E strongly increased pCaMKII levels in the cytoplasm and at surface puncta (Figures S4K and S4L). Thus, Thr287 phosphorylation of γ CaMKII likely occurs after its mobilization from the cytosol, but before dephosphorylation of Ser334.

β CaMKII Is Dispensable for γ CaMKII Translocation but Is Required for Nuclear Accumulation of pCaMKII and CaM

Upon stimulation, CaMKII isoforms other than γ CaMKII, principally β CaMKII in cultured SCG neurons, congregate at surface puncta and help initiate signaling to the nucleus (Wheeler et al., 2012). Although β CaMKII does not translocate to the nucleus (Figure S1B), its aggregation suits the role of phosphorylating γ CaMKII to enable the CaM trapping in two key respects: specific localization and activity. First, β CaMKII puncta coincided with Ca_v1 channel puncta (Wheeler et al., 2012) (Figure 5A); γ CaMKII was also mobilized to Ca_v1 channels, judging by colocalization of γ_A CaMKII S334E puncta with Ca_v1 channel puncta (Figure 5B). Second, the clusters of β CaMKII appeared to be activated, insofar as they coincided with puncta of pCaMKII (Wheeler et al., 2012), not attributable to γ CaMKII (Figures 4C,

left, and 4E, top). Thus, β CaMKII clusters appear well-suited to drive Thr287 phosphorylation of γ CaMKII.

To test this, we knocked down β CaMKII with an shRNA construct that reduced β CaMKII mRNA levels by $\sim 90\%$ while leaving γ CaMKII transcripts unchanged (Wheeler et al., 2008). The distributions of pCaMKII, γ CaMKII, and CaM were monitored in cells infected with the knockdown construct or a nonsilencing control (Figure 5C). Knockdown of β CaMKII largely abolished the K^+ -induced increase in nuclear pCaMKII (Figure 5C, top row), but spared the nuclear γ CaMKII rise (Figure 5C, second row). β CaMKII knockdown also prevented CaM translocation (Figure 5C, third row), reminiscent of the pattern seen with γ CaMKII T287A (Figures 2G, right, S2I, and S2J, right). Finally, knocking down β CaMKII also prevented CREB phosphorylation (Figure 5C, bottom row) (Wheeler et al., 2012). These observations were corroborated in pooled data (Figures S5A–S5D). Evidently, without β CaMKII-dependent phosphorylation at T287, nuclear translocation of the γ CaMKII shuttle occurs without cargo and CREB activation fails. Critically, β CaMKII shRNA resistant β CaMKII^R (Figure S5E) rescued the nuclear increase in pCaMKII, CaM translocation and pCREB response (Figure S5F–S5H), without affecting γ CaMKII nuclear translocation (Figure S5I). These observations supported the idea that β CaMKII phosphorylates γ CaMKII at Thr287 at the surface checkpoint, stabilizes the γ CaMKII–CaM complex, and thus ensures proper cotransport of Ca^{2+} /CaM to the nucleus along with γ CaMKII. Nuclear delivery of γ CaMKII is not sufficient by itself to trigger a pCREB response; cotransfer of Ca^{2+} /CaM is required.

The canonical mechanism of Thr286/287 phosphorylation, an intersubunit, intraholoenzyme reaction, was first revealed at low concentrations of CaMKII holoenzyme. However, interholoenzyme phosphorylation might occur in the concentrated environment of a Ca_v1 -centered signaling nanodomain. To test for interholoenzyme phosphorylation, we set up an enriched environment *in vitro*. The test substrate, immobilized on beads, was a γ CaMKII variant that can bind CaM but is catalytically inactive (K43R). Thr287 phosphorylation of bead-concentrated γ CaMKII K43R was significantly increased by purified β CaMKII when activated by Ca^{2+} /CaM (Figures 5D and 5E). Thus, intermolecular phosphorylation can occur if β CaMKII and γ CaMKII are colocalized in a high concentration environment.

We also tested another scenario wherein endogenous β CaMKII and γ CaMKII basally coassemble into heteromultimers and travel together to the Ca_v1 checkpoint and then to the nucleus. In contradiction, formation of near-surface puncta of β CaMKII (Figure 5F) was not accompanied by detectable puncta of γ CaMKII (Figure 5G); γ CaMKII S334E puncta verified our ability to detect puncta of γ CaMKII (Figure 5H). Furthermore, no increase in nuclear β CaMKII was detected, despite clear rises in nuclear γ CaMKII (Figures S1B and 1A). Thus, cotranslocation of fixed heteromultimers of β CaMKII and γ CaMKII was not supported. We further considered the idea that basal coassembly of β CaMKII and γ CaMKII might give way at the checkpoint to autophosphorylation-dependent subunit exchange (Stratton et al., 2014); β CaMKII could conceivably be stranded at the checkpoint while newly assembled γ CaMKII homomultimers traveled onward to the nucleus. Against this scenario, subunit exchange requires autophosphorylation of T305/T306, key residues within

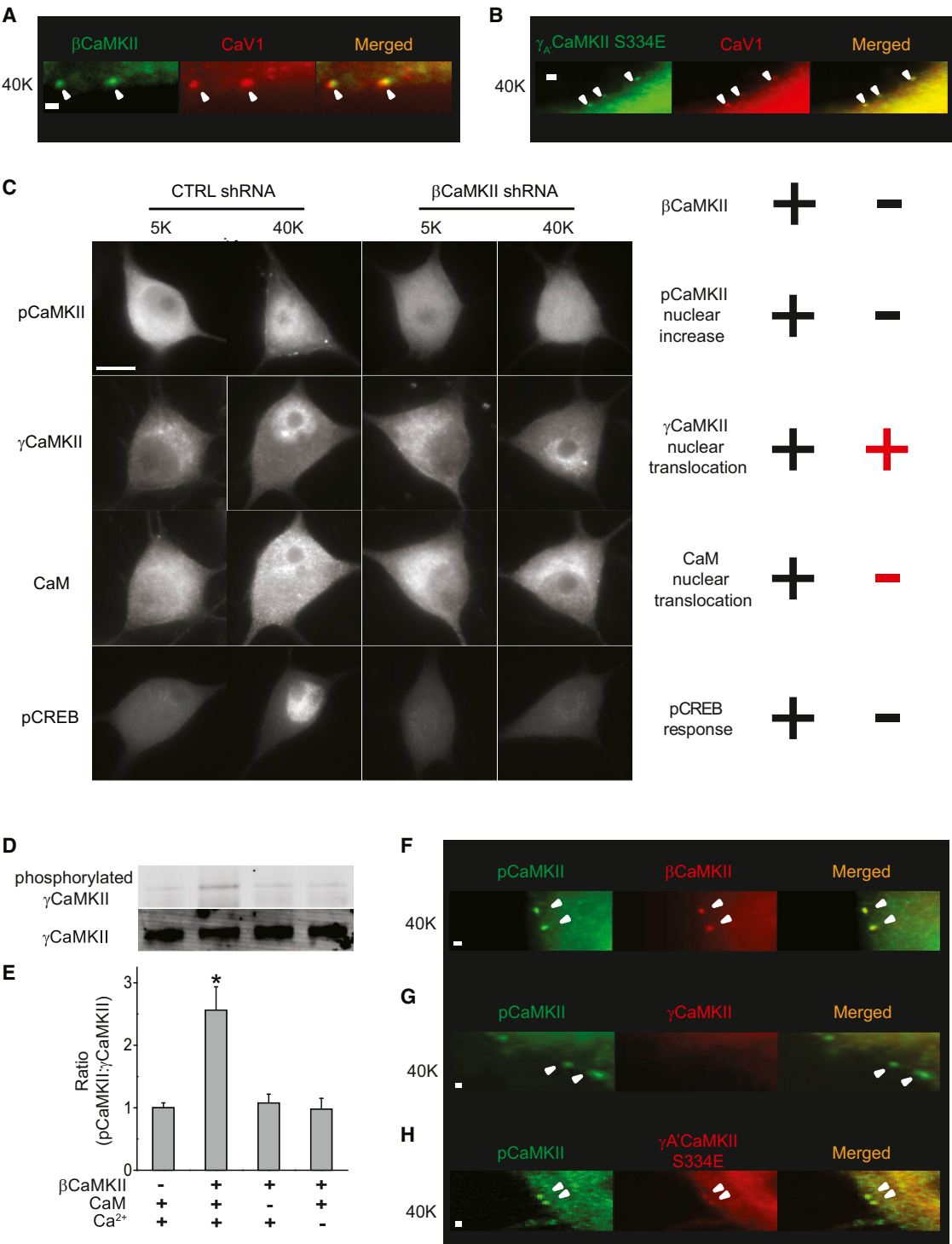


Figure 5. Phosphorylation of γ CaMKII by β CaMKII: Dispensable for γ CaMKII Translocation but Required for CaM Translocation and CREB Phosphorylation

(A and B) Arrowheads, sites where endogenous β CaMKII (A) or overexpressed γ_A CaMKII S334E (B) colocalize with puncta of Ca γ 1.3 channels upon 40 mM K⁺ stimulation for 60 s. Scale bar represents 1 μ m.

(C) SCG neurons expressing β CaMKII shRNA or nonsilencing control shRNA were stimulated with 40 mM K⁺ for 300 s and stained for pCaMKII (first row), costained for γ CaMKII and CaM (second and third row), stained for pCREB (fourth row). Scale bar represents 10 μ m. β CaMKII knockdown prevented the increase in nuclear pCaMKII levels (–), CaM translocation (–) and pCREB response (–), but did not affect γ CaMKII translocation (+). “+” and “–” indicate a significant or insignificant change respectively (see [Figures S5A–S5D](#) for details).

(legend continued on next page)

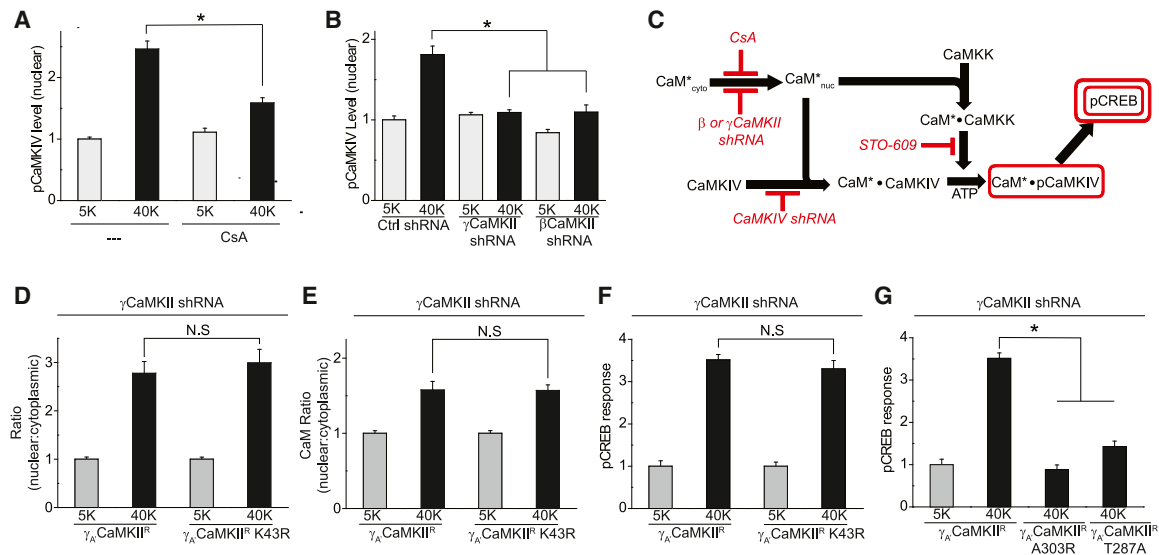


Figure 6. Activation of Nuclear CaMK Cascade and Distinct Roles of γ CaMKII and CaM in Driving CREB Phosphorylation

(A) SCG neurons stimulated with 40 mM K^+ for 10 s in the absence or presence of CaN inhibitor CsA (50 nM). Increase in nuclear pCaMKIV levels inhibited by CsA. (B) SCG neurons expressing γ CaMKII shRNA, β CaMKII shRNA or nonsilencing control shRNA were stimulated with 40 mM K^+ for 10 s and stained for pCaMKIV. Knockdown of γ CaMKII or β CaMKII prevented the activation of CaMKIV.

(C) Schema showing free Ca^{2+} /CaM (denoted CaM*) delivered by γ CaMKII activating the CaMK cascade comprised of CaMKK and CaMKIV. Prevention of critical steps by applying different inhibitors (CsA, STO-609) or shRNA (against β CaMKII, γ CaMKII or CaMKIV) indicated in red; rectangles show monitored variables (see Figure S6 for details).

(D–F) SCG neurons expressing γ CaMKII shRNA with γ CaMKII shRNA-resistant γ_A CaMKII^R or γ_A K43R were stimulated with 40 mM K^+ for 300 s (D and E) or 10 s (F). Both γ_A CaMKII^R and γ_A CaMKII^R K43R can translocate to the nucleus upon the stimulation (D), and support CaM translocation (E) and pCREB response (F). (G) SCG neurons expressing γ CaMKII shRNA with γ CaMKII shRNA resistant γ_A A303R or γ_A CaMKII^R T287A were stimulated as in (F). Neither γ_A CaMKII^R A303R nor γ_A CaMKII^R T287A rescued the pCREB response.

See also Figure S6.

the CaM footprint (Stratton et al., 2014); such autophosphorylation is mutually exclusive with Ca^{2+} /CaM binding and thus prohibited during continuous Ca^{2+} elevation (Figures 1 and S1L). Even if heteromultimers of γ CaMKII and β CaMKII form, they are unlikely to dominate γ CaMKII mobilization to either the surface membrane or the nucleus.

The γ CaMKII-CaM Shuttle Activates a Nuclear CaM Kinase Cascade

What happens once the γ CaMKII- Ca^{2+} /CaM complex arrives in the nucleus? We tested for signaling by a well-characterized nuclear “CaM kinase cascade” (Figures 6A–6C) (Means, 2000; Soderling, 1999). Nuclear-resident CaMKIV is thought to be critical for triggering CREB phosphorylation (Bito et al., 1996; Means, 2000; Soderling, 1999). CaMKIV becomes activated via Thr196 phosphorylation by CaM kinase kinase (CaMKK) (Selbert et al., 1995). The role of this cascade was probed by pharmacological

and molecular interventions and by monitoring phosphorylation of CaMKIV and CREB (shown in red in Figure 6C). CaMKIV was concentrated in the nucleus in SCG neurons and did not redistribute upon depolarization (Figures S6A and S6C). Its phosphorylation, assessed with an antibody against phospho-Thr196 CaMKIV (pCaMKIV) (Selbert et al., 1995), increased 3-fold upon K^+ -depolarization (Figures S6A and S6B). Knockdown of CaMKIV by shRNA (near-complete loss of protein; Figure S6D) abolished the depolarization-dependent increase in pCREB (Figure S6E). The specific CaMKK inhibitor STO-609 prevented the increases in nuclear pCaMKIV (Figure S6F) and pCREB (Figure S6G), confirming the involvement of CaMKK. These data show that SCG neurons rely on activation of CaMKK and CaMKIV for CREB phosphorylation.

Is cotranslocation of γ CaMKII/CaM necessary for activation of the CaMKK-CaMKIV cascade? Activation of CaMKIV was indeed prevented (1) by exposure to CsA to prevent γ CaMKII

(D and E) HA-tagged γ_A CaMKII K43R was concentrated and immobilized with agarose beads coated with HA antibody. After a 10 s exposure to 25 μ M ATP, with or without the presence of 44 μ g/ml β CaMKII, 1 mM $CaCl_2$ and 1 μ M CaM, the immobilized γ_A CaMKII K43R was eluted from the beads and collected for western blot analysis. Phosphorylation state and amount of γ_A CaMKII K43R detected by specific antibodies against pCaMKII and γ CaMKII (D). A specific antibody to β CaMKII was used to confirm that the pCaMKII was not caused by β CaMKII accumulation on the beads. (E) Ratio of pCaMKII: γ CaMKII increased significantly in the presence of β CaMKII ($n = 7$), but only if both CaM and Ca^{2+} were present ($n = 4$).

(F–H) Arrowheads indicate sites where endogenous β CaMKII (F) and overexpressed γ_A CaMKII S334E (G), but not γ CaMKII (H), colocalize with pCaMKII puncta upon 40 mM K^+ stimulation for 60 s. Scale bar represents 1 μ m.

See also Figure S5.

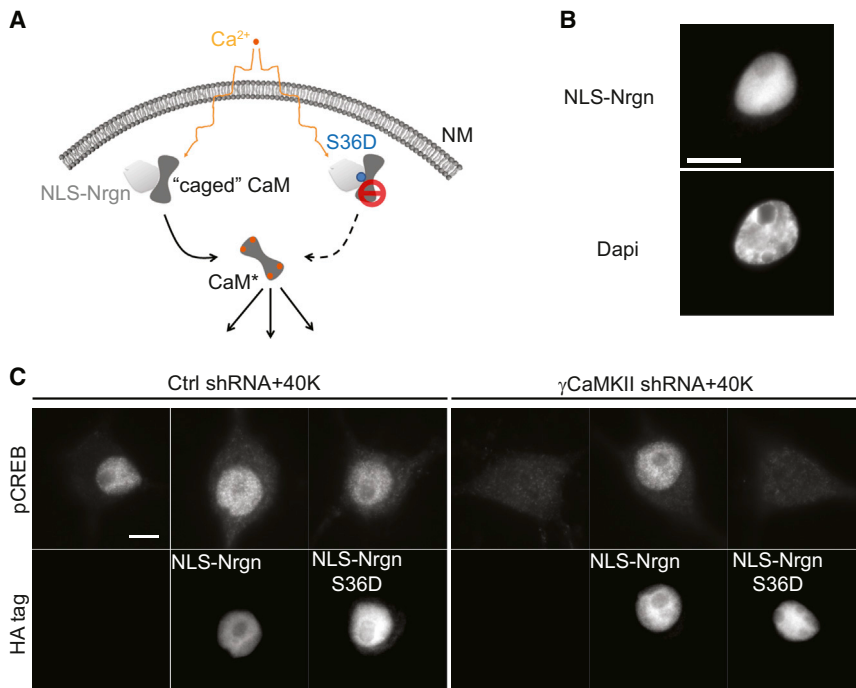


Figure 7. Nuclear Delivery of $\text{Ca}^{2+}/\text{CaM}$ Is Sufficient to Drive CREB Phosphorylation

(A) Testing the sufficiency of $\text{Ca}^{2+}/\text{CaM}$ with a nuclear-localized, caged CaM.

(B) HA-tagged NLS-Nrgn or NLS-Nrgn S36D successfully targeted to the nucleus. Scale bar represents 10 μm .

(C) SCG neurons expressing γCaMKII shRNA or nonsilencing control shRNA, stimulated with 40 mM K^+ for 10 s. NLS-Nrgn but not NLS-Nrgn S36D was able to restore the pCREB response, consistent respectively with the ability or inability to harbor CaM for release upon nuclear Ca^{2+} elevation. Under basal conditions, overexpressing NLS-Nrgn or NLS-Nrgn S36D did not affect pCREB levels (see Figures S7A and S7B for details). See also Figure S7.

also sufficient, even without γCaMKII . Nuclear liberation of CaM was accomplished by exploiting neurogranin (Nrgn), an endogenous CaM buffer that sequesters apoCaM but releases CaM once it becomes Ca^{2+} bound (Baudier et al.,

and CaM translocation (Figure 6A), (2) by shRNA knockdown of γCaMKII (Figure 6B), and (3) by βCaMKII knockdown (Figure 6B). These findings account for the inhibition of CREB phosphorylation by the same maneuvers. Activation of the nuclear CaMK cascade is the critical intermediary between γCaMKII -CaM cotransport to the nucleus and activation of CREB.

γCaMKII Catalytic Activity Is Not Necessary for CREB Phosphorylation

Does γCaMKII operate as a protein kinase or merely as a transporter of $\text{Ca}^{2+}/\text{CaM}$? To answer this, we knocked down endogenous γCaMKII with γCaMKII shRNA and compared the effects of shRNA-resistant rescue constructs, $\gamma_{\text{A}}\text{CaMKII}^{\text{R}}$ and $\gamma_{\text{A}}\text{CaMKII}^{\text{R}}$ K43R (kinase dead). The catalytically inactive protein still translocated to the nucleus (Figure 6D), rescued CaM translocation (Figure 6E), and supported the pCREB response (Figure 6F), each to the same extent as kinase active $\gamma_{\text{A}}\text{CaMKII}^{\text{R}}$. In sharp contrast, attempted rescue by expression of $\gamma_{\text{A}}\text{CaMKII}^{\text{R}}$ A303R or $\gamma_{\text{A}}\text{CaMKII}^{\text{R}}$ T287A failed to support pCREB response (Figure 6G), consistent with the inability of these variants to support respectively CaM binding or sequestration, and hence CaM translocation (Figures S2I and S4F). Indeed, inhibiting nuclear CaM untrapping from γCaMKII also prevented the pCREB response, as tested by blocking PP2A dephosphorylation of phospho- γCaMKII (see Figures S6H and S6I and legend for details). Taken together, our results indicated that nuclear $\text{Ca}^{2+}/\text{CaM}$, not the catalytic activity of γCaMKII , is necessary for triggering CREB phosphorylation.

Sufficiency of Nuclear CaM Delivery in the Absence of γCaMKII Translocation

Given the necessity of nuclear CaM delivery, over and above elevation of γCaMKII , we asked whether delivery of CaM_{nuc} is

1991). By fusing Nrgn with an N-terminal NLS, we targeted NLS-Nrgn (and thus “caged CaM”) to the nucleus of quiescent SCG neurons (Figures 7A and 7B). Expression of this construct had no effect on CREB phosphorylation without stimulation (Figures S7A and S7B) and slightly increased the pCREB response ($p < 0.03$) to depolarization (Figures 7C and S7B, left bars). In the test of sufficiency, we examined the effect of NLS-Nrgn following γCaMKII knockdown to eliminate normal cytoplasm-to-nucleus shuttling of CaM (Figure 2F). Blockade of this route of CaM delivery verifiably prevented CREB phosphorylation in 40 K^+ . In sharp contrast, the pCREB response was restored to normal levels ($p = 0.8$) by the NLS-Nrgn construct (Figures 7C and S7B, right bars). To establish that nuclear Nrgn acts to liberate $\text{Ca}^{2+}/\text{CaM}$, we tested an S36D variant of NLS-Nrgn, which lacks apoCaM binding; NLS-Nrgn S36D failed to rescue CREB phosphorylation (Figures 7C and S7B, right bars). Finally, the CaMKK inhibitor STO-609 abolished the NLS-Nrgn-rescued pCREB response (Figure S7C), confirming that the uncaged $\text{Ca}^{2+}/\text{CaM}$ operates via the nuclear CaMK cascade. This set of NLS-Nrgn experiments demonstrated that direct delivery of nuclear $\text{Ca}^{2+}/\text{CaM}$ is sufficient to drive nuclear CREB phosphorylation if the normal shuttling of CaM is disabled. Thus, nuclear $\text{Ca}^{2+}/\text{CaM}$ is both necessary and sufficient to support this form of E-T coupling.

DISCUSSION

Our experiments demonstrate a mechanism for transmitting information within cells: shuttling $\text{Ca}^{2+}/\text{CaM}$ from one location to another. γCaMKII , largely overlooked in neuroscience since its discovery 25 years ago (Tobimatsu et al., 1988), is identified here as the surface-to-nucleus shuttle in sympathetic and neocortical pyramidal neurons. The shuttle works as follows: Neuronal

membrane depolarization opens Ca_v1 channels that deliver Ca^{2+} to the cytoplasm and promote binding of $\text{Ca}^{2+}/\text{CaM}$ to γCaMKII . The $\text{Ca}^{2+}/\text{CaM}-\gamma\text{CaMKII}$ complex is recruited to Ca_v1 channels where another isoform of CaMKII (βCaMKII in sympathetic neurons, α , βCaMKII in cortical neurons) also clusters. Two regulatory events ensue: the phosphorylation of γCaMKII at T287 by βCaMKII , trapping the $\text{Ca}^{2+}/\text{CaM}$ cargo, and the CaN-mediated dephosphorylation of γCaMKII at S334, enabling an adjacent NLS to direct the loaded shuttle to the nucleus. Nuclear delivery of $\text{Ca}^{2+}/\text{CaM}$ activates the nuclear CaMK cascade, thus driving CREB phosphorylation and transcription of CRE-regulated genes (Graphical Abstract).

Clarifying How $\text{Ca}^{2+}/\text{CaM}$ Translocation Serves as a Long-Range Communication Mechanism

CaM movements from cytoplasm to nucleus upon elevation of $[\text{Ca}^{2+}]_{\text{cyto}}$ have previously been reported in neurons (Deisseroth et al., 1998), mammalian cell lines (Teruel et al., 2000; Thorogate and Török, 2004), and heart cells (Wu and Bers, 2007). Skepticism about the functional relevance of these observations has persisted (Hagenston and Bading, 2011; Hardingham et al., 2001). The abundance of nuclear CaM may seem to obviate any need for CaM translocation. However, nuclear free CaM is in short supply (Teruel et al., 2000) because of the abundance of nuclear CaM-binding proteins (Bachs et al., 1994), leaving opportunity for freshly imported $\text{Ca}^{2+}/\text{CaM}$ to drive further signaling (Teruel et al., 2000). Another concern is the putatively rapid dissociation of Ca^{2+} from CaM once $[\text{Ca}^{2+}]_{\text{free}}$ begins to fall. It has been unclear how CaM, lacking an NLS, might travel to the nucleus other than by passive diffusion (Thorogate and Török, 2004). We proposed that $\text{Ca}^{2+}/\text{CaM}$ stabilization and nuclear targeting could both arise from binding to a CaMK, but were unable to find such a partner (Deisseroth et al., 1998; Mermelstein et al., 2001). These issues are now resolved by the identification of γCaMKII as the long-sought molecular shuttle.

Functional Rationale of CaM-Driven Signaling

The shuttle mechanism helps clarify the functional logic of excitation-pCREB coupling. Clusters of Ca_v1 channels provide a nucleation point for participants in surface-to-nucleus communication, including CaN and βCaMKII (Wheeler et al., 2008, 2012), thus illuminating the long-observed reliance of E-T coupling on Ca_v1 channels (Deisseroth et al., 1996; Greenberg et al., 1986; Murphy et al., 1991; Wheeler et al., 2012). The joint involvement of βCaMKII and calcineurin accounts for previously puzzling findings that CaM kinase and CaN work synergistically rather than in opposition to promote CREB phosphorylation (Hahn et al., 2003) and CRE-mediated gene expression (Kingsbury et al., 2007; Schwaninger et al., 1995). The localization of multiple signaling events within the nanodomain of Ca_v1 channels accounts for differential effects of fast and slow on-rate Ca^{2+} buffers (BAPTA, EGTA) in preventing CaMKII relocation (Wheeler et al., 2012) and CREB phosphorylation (Deisseroth et al., 1996). Launching the signaling at a Ca_v1 -centered Ca^{2+} nanodomain frees up separate clusters of Ca_v2 channels for other functions such as signaling to ER and mitochondria (Wheeler et al., 2012). By temporarily trapping $\text{Ca}^{2+}/\text{CaM}$, a shuttle mechanism can go on signaling even after rises in cytosolic Ca^{2+} have sub-

sided, thus reducing the duration of Ca^{2+} elevation needed to trigger a response. Whether similar “private line” communication also holds for the wide array of Ca^{2+} entry and release pathways within cells (Berridge, 2012; Clapham, 2007) requires further investigation.

Our experiments indicate that γCaMKII serves to sequester and convey $\text{Ca}^{2+}/\text{CaM}$, and its kinase activity is dispensable for driving CREB phosphorylation. Progressive accumulation of nuclear $\text{Ca}^{2+}/\text{CaM}$ provides a means for integrating the effects of multiple weak stimuli (Mermelstein et al., 2001). Because CaMKK and CaMKIV both require $\text{Ca}^{2+}/\text{CaM}$ binding to drive CaMKIV activation (Means, 2000; Wayman et al., 2008), CREB phosphorylation should increase in a steep power law relationship with $\Delta[\text{Ca}^{2+}/\text{CaM}]_{\text{nuc}}$, consistent with our data. Activation of nuclear CaMKIV has multiple regulatory effects beyond CREB phosphorylation. CaMKIV-mediated phosphorylation activates CREB binding protein (CPB) (Impey et al., 2002), an important cofactor of CREB, CREST and other transcription factors. CBP also regulates the nuclear localization of certain histone deacetylases (McKinsey et al., 2000). Furthermore, CaMKIV helps control alternative splicing of pre-mRNA (Xie and Black, 2001). Thus, by clarifying how nuclear CaMKIV becomes activated, our findings help explain the dominant role of Ca_v1 channels in phenomena ranging from activation of CBP to histone deacetylation and exon selection.

Higher-Order Significance and Distinctions from Other Pathways

The importance of nuclear CaM for brain function has been shown with a nucleus-localized trap that curbs rises in nuclear $\text{Ca}^{2+}/\text{CaM}$ while sparing cytosolic CaM signaling. This inhibited CREB phosphorylation, curbed L-LTP, and abrogated spatial memory (Limbäck-Stokin et al., 2004); thus functional consequences of thwarting the $\text{Ca}^{2+}/\text{CaM}$ shuttle were elegantly revealed. This CaM/CaMK-based system adds to known mechanisms for signaling between neuronal (e.g., postsynaptic) membrane and nucleus (Ch'ng and Martin, 2011; Hagenston and Bading, 2011; Jordan and Kreutz, 2009; Saha and Dudek, 2008). The present mechanism likely tracks neuronal depolarization rather than synaptic activity per se, as is likely for the NMDAR-driven transcription factors NF κ B (Meffert et al., 2003), Jacob (Karpova et al., 2013) and CRT1/TORC1 (Ch'ng et al., 2012). These systems may link specific inputs to a restricted set of transcriptional events. In contrast, translocation of $\text{Ca}^{2+}/\text{CaM}$ and activation of CaMKIV may achieve a broader impact because of the multiplicity of CaMKIV actions. Of known pathways, the CaM kinase-based mechanism is quickest to activate and most sensitive to brief, weak stimuli; even 50 spikes will trigger a 50% activation of CREB over basal levels (Wheeler et al., 2012). Thus, the shuttle mechanism may be tuned for efficacy, speed and sensitivity.

Implications for Schizophrenia, Autism, and Other Neuropsychiatric Disorders

Several proteins in the shuttle pathway (subunits of Ca_v1 channels, γCaMKII , βCaMKII , and CaN) are encoded by genes associated with major neuropsychiatric disorders (autism spectrum disorder [ASD], schizophrenia [SCZ], major depressive disorder

[MDD], and bipolar disorder [BPD]) (Table S1; Supplemental Information). Further study is needed to determine which genetic modifications are causal. Already, the extensive representation of the signaling components described here supports the notion that altered activity-dependent regulation of nuclear events may be a general hallmark of mental disorders. For example, *CaMK2G*, the gene for γ CaMKII, crops up repeatedly in neuropsychiatric studies. A polymorphism in *CaMK2G* is strongly related to variability in human memory performance (de Quervain and Papassotiropoulos, 2006). Protein levels of γ CaMKII (and of β CaMKII) appear significantly elevated in the lateral habenulae of rat models of MDD (Li et al., 2013). Likewise, the abundance of γ CaMKII protein is increased in NMDAR-related mouse models of schizophrenia (Table S1) (Kocerha et al., 2009). Finally, *CaMK2G* is a member of a cluster of genes (M12) that has been implicated in autism by transcriptome analysis of autistic brains. Alternative splicing of *CaMK2G* is sharply altered in ASD samples (Voineagu et al., 2011); this occurs in association with dysregulation of A2BP1, a splicing factor regulated by CaMKIV (Xie and Black, 2001). Thus, our findings could be relevant to brain disorders in multiple ways: by identification of signaling molecules that support CaMKIV-driven alternative splicing as well as activity-dependent transcription.

EXPERIMENTAL PROCEDURES

Additional information regarding primary cultures, plasmids, buffers, antibodies, primer sequences, sample preparation, mass spectrometry analysis, and detailed procedures is provided in the Extended Experimental Procedures.

Primary Neuronal Cultures

SCG neurons or cortical neurons were cultured as previously described (Wheeler et al., 2008, 2012), with minor modifications (see Extended Experimental Procedures).

Drug Treatments and Stimulation

We stimulated SCG or cortical neurons with the indicated K solution at 37°C for 10–300 s before fixation (see Extended Experimental Procedures).

Lentiviral Transduction of SCG Neurons

Lentiviral constructs were made with psPAX2 and pMD2.g. Lentivirus was added to SCG cultures 1 day after plating, using GFP expression to monitor infection (see Extended Experimental Procedures).

Image Analysis

Images for pCREB quantification and puncta weight were analyzed as previously described (Wheeler et al., 2012).

Immunoprecipitation

Pierce Classic IP Kit (Thermo Fisher) was used to concentrate γ CaMKII K43R on agarose beads, the degree of phosphorylation, and the total amount of γ CaMKII K43R was determined by western blot.

Statistical Analysis

All the data were normalized to corresponding basal conditions. Without further indication, quantification was based on ≥ 24 fields under a 63 \times objective from three to six platings per condition.

SUPPLEMENTAL INFORMATION

Supplemental Information includes Extended Experimental Procedures, seven figures, and one table and can be found with this article online at <http://dx.doi.org/10.1016/j.cell.2014.09.019>.

AUTHOR CONTRIBUTIONS

H.M. and R.W.T. conceived the project. R.D.G., J.F.E., and H.M. designed the constructs. R.D.G. designed the shRNA and did the RT-PCR. B.L. prepared samples for mass spectrometry. G.Z., E.T., and T.A.N. performed mass spectrometry analysis. S.M.C. and B.L. did the experiments in cortical neurons. H.M. performed all the other experiments. H.M. and R.W.T. wrote the manuscript with comments from all of the other authors.

ACKNOWLEDGMENTS

We thank Gord Fishell, Andy Hudmon, Paul De Koninck, Niels Ringstad, and Michael Tadmor for insightful comments on an earlier manuscript and Steven Burden for valuable suggestions. We thank Kathleen Morgan and Cynthia Gallant for their support at initial stages. We also thank Tsien laboratory members for discussions throughout the execution of this project. This work was supported by research grants to R.W.T. from the National Institute of General Medical Sciences (GM058234), the National Institute of Neurological Disorders and Stroke (NS24067), the National Institute of Mental Health (MH071739), and the Simons, Mathers, and Burnett Family Foundations. S.C. is supported by a Medical Scientist Training Program Fellowship. The Neubert laboratory is supported by the NIH (NP30 NS050276 and S10 RR027990 to T.A.N.).

Received: February 18, 2014

Revised: July 2, 2014

Accepted: September 9, 2014

Published: October 9, 2014

REFERENCES

- Bachs, O., Agell, N., and Carafoli, E. (1994). Calmodulin and calmodulin-binding proteins in the nucleus. *Cell Calcium* 16, 289–296.
- Bartsch, D., Casadio, A., Karl, K.A., Serodio, P., and Kandel, E.R. (1998). CREB1 encodes a nuclear activator, a repressor, and a cytoplasmic modulator that form a regulatory unit critical for long-term facilitation. *Cell* 95, 211–223.
- Baudier, J., Deloulme, J.C., Van Dorsselaer, A., Black, D., and Matthes, H.W. (1991). Purification and characterization of a brain-specific protein kinase C substrate, neurogranin (p17). Identification of a consensus amino acid sequence between neurogranin and neuromodulin (GAP43) that corresponds to the protein kinase C phosphorylation site and the calmodulin-binding domain. *J. Biol. Chem.* 266, 229–237.
- Bayer, K.U., Löhler, J., Schulman, H., and Harbers, K. (1999). Developmental expression of the CaM kinase II isoforms: ubiquitous gamma- and delta-CaM kinase II are the early isoforms and most abundant in the developing nervous system. *Brain Res. Mol. Brain Res.* 70, 147–154.
- Berridge, M.J. (2012). Calcium signalling remodelling and disease. *Biochem. Soc. Trans.* 40, 297–309.
- Bitto, H., Deisseroth, K., and Tsien, R.W. (1996). CREB phosphorylation and dephosphorylation: a Ca(2+)- and stimulus duration-dependent switch for hippocampal gene expression. *Cell* 87, 1203–1214.
- Ch'ng, T.H., and Martin, K.C. (2011). Synapse-to-nucleus signaling. *Curr. Opin. Neurobiol.* 21, 345–352.
- Ch'ng, T.H., Uzgil, B., Lin, P., Avliyakulov, N.K., O'Dell, T.J., and Martin, K.C. (2012). Activity-dependent transport of the transcriptional coactivator CRTC1 from synapse to nucleus. *Cell* 150, 207–221.
- Clapham, D.E. (2007). Calcium signaling. *Cell* 131, 1047–1058.
- de Ligt, J., Willemsen, M.H., van Bon, B.W., Kleefstra, T., Yntema, H.G., Kroes, T., Vulto-van Silfhout, A.T., Koolen, D.A., de Vries, P., Gilissen, C., et al. (2012). Diagnostic exome sequencing in persons with severe intellectual disability. *N. Engl. J. Med.* 367, 1921–1929.
- de Quervain, D.J., and Papassotiropoulos, A. (2006). Identification of a genetic cluster influencing memory performance and hippocampal activity in humans. *Proc. Natl. Acad. Sci. USA* 103, 4270–4274.

- Deisseroth, K., Bito, H., and Tsien, R.W. (1996). Signaling from synapse to nucleus: postsynaptic CREB phosphorylation during multiple forms of hippocampal synaptic plasticity. *Neuron* 16, 89–101.
- Deisseroth, K., Heist, E.K., and Tsien, R.W. (1998). Translocation of calmodulin to the nucleus supports CREB phosphorylation in hippocampal neurons. *Nature* 392, 198–202.
- Deisseroth, K., Mermelstein, P.G., Xia, H., and Tsien, R.W. (2003). Signaling from synapse to nucleus: the logic behind the mechanisms. *Curr. Opin. Neurobiol.* 13, 354–365.
- Dolmetsch, R.E., Pajvani, U., Fife, K., Spotts, J.M., and Greenberg, M.E. (2001). Signaling to the nucleus by an L-type calcium channel-calmodulin complex through the MAP kinase pathway. *Science* 294, 333–339.
- Gangopadhyay, S.S., Barber, A.L., Gallant, C., Grabarek, Z., Smith, J.L., and Morgan, K.G. (2003). Differential functional properties of calmodulin-dependent protein kinase II gamma variants isolated from smooth muscle. *Biochem. J.* 372, 347–357.
- Giese, K.P., Fedorov, N.B., Filipkowski, R.K., and Silva, A.J. (1998). Autophosphorylation at Thr286 of the alpha calcium-calmodulin kinase II in LTP and learning. *Science* 279, 870–873.
- Greenberg, M.E., Ziff, E.B., and Greene, L.A. (1986). Stimulation of neuronal acetylcholine receptors induces rapid gene transcription. *Science* 234, 80–83.
- Hagenston, A.M., and Bading, H. (2011). Calcium signaling in synapse-to-nucleus communication. *Cold Spring Harb. Perspect. Biol.* 3, a004564.
- Hahn, S.H., Chen, Y., Vinson, C., and Eiden, L.E. (2003). A calcium-initiated signaling pathway propagated through calcineurin and cAMP response element-binding protein activates proenkephalin gene transcription after depolarization. *Mol. Pharmacol.* 64, 1503–1511.
- Hardingham, G.E., Arnold, F.J., and Bading, H. (2001). Nuclear calcium signaling controls CREB-mediated gene expression triggered by synaptic activity. *Nat. Neurosci.* 4, 261–267.
- Heist, E.K., Srinivasan, M., and Schulman, H. (1998). Phosphorylation at the nuclear localization signal of Ca²⁺/calmodulin-dependent protein kinase II blocks its nuclear targeting. *J. Biol. Chem.* 273, 19763–19771.
- Hudmon, A., and Schulman, H. (2002). Neuronal Ca²⁺/calmodulin-dependent protein kinase II: the role of structure and autoregulation in cellular function. *Annu. Rev. Biochem.* 71, 473–510.
- Hudmon, A., Lebel, E., Roy, H., Sik, A., Schulman, H., Waxham, M.N., and De Koninck, P. (2005). A mechanism for Ca²⁺/calmodulin-dependent protein kinase II clustering at synaptic and nonsynaptic sites based on self-association. *J. Neurosci.* 25, 6971–6983.
- Impey, S., Mark, M., Villacres, E.C., Poser, S., Chavkin, C., and Storm, D.R. (1996). Induction of CRE-mediated gene expression by stimuli that generate long-lasting LTP in area CA1 of the hippocampus. *Neuron* 16, 973–982.
- Impey, S., Fong, A.L., Wang, Y., Cardinaux, J.R., Fass, D.M., Obrietan, K., Wayman, G.A., Storm, D.R., Soderling, T.R., and Goodman, R.H. (2002). Phosphorylation of CBP mediates transcriptional activation by neural activity and CaM kinase IV. *Neuron* 34, 235–244.
- Jordan, B.A., and Kreutz, M.R. (2009). Nucleocytoplasmic protein shuttling: the direct route in synapse-to-nucleus signaling. *Trends Neurosci.* 32, 392–401.
- Kandel, E.R. (2001). The molecular biology of memory storage: a dialogue between genes and synapses. *Science* 294, 1030–1038.
- Karpova, A., Mikhaylova, M., Bera, S., Bär, J., Reddy, P.P., Behnisch, T., Rankovic, V., Spilker, C., Bethge, P., Sahin, J., et al. (2013). Encoding and transducing the synaptic or extrasynaptic origin of NMDA receptor signals to the nucleus. *Cell* 152, 1119–1133.
- Kennedy, M.B. (2000). Signal-processing machines at the postsynaptic density. *Science* 290, 750–754.
- Kingsbury, T.J., Bambrick, L.L., Roby, C.D., and Krueger, B.K. (2007). Calcineurin activity is required for depolarization-induced, CREB-dependent gene transcription in cortical neurons. *J. Neurochem.* 103, 761–770.
- Kocerha, J., Faghihi, M.A., Lopez-Toledano, M.A., Huang, J., Ramsey, A.J., Caron, M.G., Sales, N., Willoughby, D., Elmen, J., Hansen, H.F., et al. (2009). MicroRNA-219 modulates NMDA receptor-mediated neurobehavioral dysfunction. *Proc. Natl. Acad. Sci. USA* 106, 3507–3512.
- Li, K., Zhou, T., Liao, L., Yang, Z., Wong, C., Henn, F., Malinow, R., Yates, J.R., 3rd, and Hu, H. (2013). β CaMKII in lateral habenula mediates core symptoms of depression. *Science* 341, 1016–1020.
- Limbäck-Stokin, K., Korzus, E., Nagaoka-Yasuda, R., and Mayford, M. (2004). Nuclear calcium/calmodulin regulates memory consolidation. *J. Neurosci.* 24, 10858–10867.
- Lisman, J., Schulman, H., and Cline, H. (2002). The molecular basis of CaMKII function in synaptic and behavioural memory. *Nat. Rev. Neurosci.* 3, 175–190.
- Lonze, B.E., and Ginty, D.D. (2002). Function and regulation of CREB family transcription factors in the nervous system. *Neuron* 35, 605–623.
- Ma, H., Cohen, S., Li, B., and Tsien, R.W. (2012). Exploring the dominant role of Cav1 channels in signalling to the nucleus. *Biosci. Rep.* 33, 97–101.
- Malinow, R., Schulman, H., and Tsien, R.W. (1989). Inhibition of postsynaptic PKC or CaMKII blocks induction but not expression of LTP. *Science* 245, 862–866.
- McKinsey, T.A., Zhang, C.L., Lu, J., and Olson, E.N. (2000). Signal-dependent nuclear export of a histone deacetylase regulates muscle differentiation. *Nature* 408, 106–111.
- Means, A.R. (2000). Regulatory cascades involving calmodulin-dependent protein kinases. *Mol. Endocrinol.* 14, 4–13.
- Meffert, M.K., Chang, J.M., Wiltgen, B.J., Fanselow, M.S., and Baltimore, D. (2003). NF-kappa B functions in synaptic signaling and behavior. *Nat. Neurosci.* 6, 1072–1078.
- Mermelstein, P.G., Deisseroth, K., Dasgupta, N., Isaksen, A.L., and Tsien, R.W. (2001). Calmodulin priming: nuclear translocation of a calmodulin complex and the memory of prior neuronal activity. *Proc. Natl. Acad. Sci. USA* 98, 15342–15347.
- Meyer, T., Hanson, P.I., Stryer, L., and Schulman, H. (1992). Calmodulin trapping by calcium-calmodulin-dependent protein kinase. *Science* 256, 1199–1202.
- Morgan, J.I., and Curran, T. (1986). Role of ion flux in the control of c-fos expression. *Nature* 322, 552–555.
- Murphy, T.H., Worley, P.F., and Baraban, J.M. (1991). L-type voltage-sensitive calcium channels mediate synaptic activation of immediate early genes. *Neuron* 7, 625–635.
- Saha, R.N., and Dudek, S.M. (2008). Action potentials: to the nucleus and beyond. *Exp. Biol. Med.* (Maywood) 233, 385–393.
- Schwaninger, M., Blume, R., Krüger, M., Lux, G., Oetjen, E., and Knepel, W. (1995). Involvement of the Ca(2+)-dependent phosphatase calcineurin in gene transcription that is stimulated by cAMP through cAMP response elements. *J. Biol. Chem.* 270, 8860–8866.
- Selbert, M.A., Anderson, K.A., Huang, Q.H., Goldstein, E.G., Means, A.R., and Edelman, A.M. (1995). Phosphorylation and activation of Ca(2+)-calmodulin-dependent protein kinase IV by Ca(2+)-calmodulin-dependent protein kinase Ia kinase. Phosphorylation of threonine 196 is essential for activation. *J. Biol. Chem.* 270, 17616–17621.
- Shen, K., and Meyer, T. (1999). Dynamic control of CaMKII translocation and localization in hippocampal neurons by NMDA receptor stimulation. *Science* 284, 162–166.
- Sheng, M., McFadden, G., and Greenberg, M.E. (1990). Membrane depolarization and calcium induce c-fos transcription via phosphorylation of transcription factor CREB. *Neuron* 4, 571–582.
- Silva, A.J., Stevens, C.F., Tonegawa, S., and Wang, Y. (1992). Deficient hippocampal long-term potentiation in alpha-calcium-calmodulin kinase II mutant mice. *Science* 257, 201–206.
- Soderling, T.R. (1999). The Ca-calmodulin-dependent protein kinase cascade. *Trends Biochem. Sci.* 24, 232–236.

- Stratton, M., Lee, I.H., Bhattacharyya, M., Christensen, S.M., Chao, L.H., Schulman, H., Groves, J.T., and Kuriyan, J. (2014). Correction: Activation-triggered subunit exchange between CaMKII holoenzymes facilitates the spread of kinase activity. *eLife* 3, e02490.
- Takeuchi, M., and Fujisawa, H. (1998). New alternatively spliced variants of calmodulin-dependent protein kinase II from rabbit liver. *Gene* 221, 107–115.
- Takeuchi, Y., Fukunaga, K., and Miyamoto, E. (2002). Activation of nuclear Ca(2+)/calmodulin-dependent protein kinase II and brain-derived neurotrophic factor gene expression by stimulation of dopamine D2 receptor in transfected NG108-15 cells. *J. Neurochem.* 82, 316–328.
- Teruel, M.N., Chen, W., Persechini, A., and Meyer, T. (2000). Differential codes for free Ca(2+)-calmodulin signals in nucleus and cytosol. *Curr. Biol.* 10, 86–94.
- Thorogate, R., and Török, K. (2004). Ca²⁺-dependent and -independent mechanisms of calmodulin nuclear translocation. *J. Cell Sci.* 117, 5923–5936.
- Tobimatsu, T., and Fujisawa, H. (1989). Tissue-specific expression of four types of rat calmodulin-dependent protein kinase II mRNAs. *J. Biol. Chem.* 264, 17907–17912.
- Tobimatsu, T., Kameshita, I., and Fujisawa, H. (1988). Molecular cloning of the cDNA encoding the third polypeptide (gamma) of brain calmodulin-dependent protein kinase II. *J. Biol. Chem.* 263, 16082–16086.
- Voineagu, I., Wang, X., Johnston, P., Lowe, J.K., Tian, Y., Horvath, S., Mill, J., Cantor, R.M., Blencowe, B.J., and Geschwind, D.H. (2011). Transcriptomic analysis of autistic brain reveals convergent molecular pathology. *Nature* 474, 380–384.
- Wayman, G.A., Lee, Y.S., Tokumitsu, H., Silva, A.J., and Soderling, T.R. (2008). Calmodulin-kinases: modulators of neuronal development and plasticity. *Neuron* 59, 914–931.
- Wheeler, D.G., Barrett, C.F., Groth, R.D., Safa, P., and Tsien, R.W. (2008). CaMKII locally encodes L-type channel activity to signal to nuclear CREB in excitation-transcription coupling. *J. Cell Biol.* 183, 849–863.
- Wheeler, D.G., Groth, R.D., Ma, H., Barrett, C.F., Owen, S.F., Safa, P., and Tsien, R.W. (2012). Ca(V)1 and Ca(V)2 channels engage distinct modes of Ca(2+) signaling to control CREB-dependent gene expression. *Cell* 149, 1112–1124.
- Wu, X., and Bers, D.M. (2007). Free and bound intracellular calmodulin measurements in cardiac myocytes. *Cell Calcium* 41, 353–364.
- Wu, G.Y., Deisseroth, K., and Tsien, R.W. (2001). Activity-dependent CREB phosphorylation: convergence of a fast, sensitive calmodulin kinase pathway and a slow, less sensitive mitogen-activated protein kinase pathway. *Proc. Natl. Acad. Sci. USA* 98, 2808–2813.
- Xie, J., and Black, D.L. (2001). A CaMK IV responsive RNA element mediates depolarization-induced alternative splicing of ion channels. *Nature* 410, 936–939.
- Yin, J.C., Del Vecchio, M., Zhou, H., and Tully, T. (1995). CREB as a memory modulator: induced expression of a dCREB2 activator isoform enhances long-term memory in *Drosophila*. *Cell* 81, 107–115.

EXTENDED EXPERIMENTAL PROCEDURES

Primary Cultures of SCG or Cortical Neurons

SCG neurons were cultured from postnatal day 0 to 1 Sprague-Dawley rat pups as previously described (Wheeler et al., 2008), using a protocol approved by the Institutional Animal Care and Use Committees at Stanford University and at New York University. Following their dissection, SCG neurons were incubated for 30 min at 37°C in a solution containing 15 mg/ml trypsin (Sigma). Cells were then washed, dissociated by trituration with a fire-polished, siliconized Pasteur pipette and plated on laminin/poly-D-lysine-coated glass coverslips (BD Biosciences) in 24-well plates. The cultures were maintained in 5% CO₂ at 37°C in L-15 medium (Invitrogen) supplemented with sodium bicarbonate, penicillin/streptomycin, glucose, 10% fetal bovine serum, 25 ng/ml nerve growth factor and a vitamin mix (Hawrot and Patterson, 1979). Cultures were fed one day after plating by replacing half the medium with medium containing cytosine arabinoside (5 μM). In all experiments, neurons were used 4–5 days after plating.

Cortical neurons were cultured from postnatal day 0 to 1 Sprague-Dawley rat pups. The frontal cortex was isolated and washed twice in ice-cold modified HBSS (4.2 mM NaHCO₃ and 1 mM HEPES, pH 7.35, 300 mOsm) containing 20% fetal bovine serum (FBS; Hyclone, Logan, UT). Cortices were washed and digested for 30 min in a papain solution (2.5 ml HBSS + 145 U papain + 40 μl DNase) at 37°C with gentle shaking every 10 min. Digestion was stopped by adding 5 ml of modified HBSS containing 20% fetal bovine serum. After additional washing, the tissue was dissociated using Pasteur pipettes of decreasing diameter. The cell suspension was pelleted twice and filtered with a 70 μm nylon strainer, and plated on 10 mm coverslips coated with poly-D-lysine. The cultures were maintained in NbActiv4 (BrainBits, Springfield, IL). A 50% medium change was performed at 7 days, and once per week thereafter. Neurons were used 13–15 days after plating.

Drug Treatments and Stimulation

To induce CREB phosphorylation, we stimulated SCG or cortical neurons with the indicated high [K⁺] solution at 37°C for 10 to 300 s, and fixed the cells immediately after the stimulation (in 4% paraformaldehyde in PBS, with 20 mM EGTA and 4% (w/v) sucrose). Where indicated, drugs were added 30 min before and included throughout the stimulation. All K⁺-rich stimulation solutions contained 0.5 μM TTX (Ascent Scientific) to block action potentials. In addition, when stimulating cortical neurons, 10 μM NBQX (Ascent Scientific) and 10 μM APV (Ascent Scientific) were included to block AMPA and NMDA receptors, respectively. 5 mM K Tyrode's consisted of (in mM): 150 NaCl, 5 KCl, 2 MgCl₂, 2 CaCl₂, 10 HEPES, 10 glucose, pH 7.4. When stimulating with elevated [K⁺], Na⁺ was adjusted to maintain osmolality.

DNA Constructs

pCDH-EF1α-HA-tagged-γ_ACaMKII

Human *CaMK2G* was PCR amplified using a cDNA clone as template (clone ID 4813948, Thermo Scientific) with primers containing an HA tag and restriction sites for subcloning into the pCDH-EF1α-MCS-T2A-copGFP construct (Systems Biosciences); T2A-copGFP was removed in the process of HA-γ_ACaMKII insertion. The HA-tagged γ_ACaMKII construct was generated by PCR amplification of the HA-γ_ACaMKII construct with primers to delete the 21 amino acids between residues 316 and 336 present in γ_ACaMKII but absent in γ_ACaMKII.

pCDH-EF1α-HA-tagged-NLS-Nrgn

Neurogranin was PCR amplified from a rat cDNA library using primers to add a NLS and was subcloned into the pCR2.1 vector by topoisomerase reaction (Life Technologies). The resulting construct was used as template in PCR with primers to add an HA tag and was then subcloned into the pCDH-EF1α-MCS-T2A-copGFP construct (Systems Biosciences) to produce pCDH-EF1α-HA-NLS-Nrgn.

pCDH-EF1α-AcGFP-γ_ACaMKII

AcGFP (monomeric GFP) was PCR amplified from pAcGFP-LRRK2 (Addgene) and subcloned into the pCDH-EF1α-HA-tagged-γ_ACaMKII, replacing the HA tag.

Point mutations were produced using QuikChange Lightning Site Directed Mutagenesis Kit (Agilent) with pCDH-EF1α-HA-γ_ACaMKII or pCDH-EF1α-HA-NLS-Nrgn as template and the following primer and its reverse-complement for each point mutation (mutated bases in lower case bold):

γ_ACaMKII S334E: G AAG TCG GAT GGC GGT GTC AAG AAA AGG AAG **ga**G AGT TCC AGC GTG CAC CTA ATG GAG CC

γ_ACaMKII A303R: GG AGA AAA CTG AAG GGT **cg**C ATC CTC ACG ACC ATG C

γ_ACaMKII K43R: CG CAG GAG TAC GCA GCA **Ag**A ATC ATC AAT ACC AAG AA

NLS-Nrgn S36D: CA GCC AAA ATC CAG GCG **ga**t TTT CGG GGC CAC ATG G

For knockdown of γCaMKII, we designed three separate shRNAs against γCaMKII and evaluated each one empirically in HEK293 cells for their ability to knockdown overexpressed human γCaMKII. For each shRNA, two complementary DNA oligonucleotides (Eurofins MWG Operon, Huntsville, AL) were annealed to produce a double-stranded DNA fragment encoding a 19-nucleotide sense strand (uppercase), 9-nucleotide loop (lowercase italicized), and 19-nucleotide antisense strand (uppercase) of the γCaMKII sequence. The sequence of the most efficacious shRNA modified (bold) to target rat γCaMKII, "γCaMKII shRNA 2" is as follows: 5'-cgc gtc ccc TGG CCT **GGC** CAT CGA AGT **GCA** *ttc aag aga* TGC ACT TCG ATG **GCC** AGG CCA ttt ttg gaa at-3' and 5'-cga ttt cca aaa aTG GCC **TGG** CCA TCG AAG **TGC** *Atc tct tga* aTG TAC TTC GAT GGC TAG GCC Agg gga-3'. The annealed γCaMKII

shRNA was then subcloned into the *MluI* and *ClaI* sites of the pLVTHM vector. Since all the γ CaMKII cDNA constructs used in this study are based on the human γ CaMKII sequence, they are resistant to rat γ CaMKII shRNA because of two bases of difference from the shRNA target sequence (γ CaMKII^R). The pLVTHM lentiviral vectors containing β CaMKII-shRNA, or the nonsilencing shRNA were described previously (Wheeler et al., 2008). An shRNA resistant β CaMKII cDNA was generated using the QuikChange Lightning Site-Directed Mutagenesis Kit (Agilent) with the primers 5'-CAAGCTCTGCACCGGCCATGAATACGCCCAAGATCATTAAACACCAA GAAG-3' and its reverse complement to create 4 silent bp changes in the shRNA target sequence (from GAGTATGCAGCTAAGATCA to GAATACGCCCAAGATCA). The coding sequence of this resistant cDNA (minus the start codon) was then generated by PCR using the following primers: TCTAGAGCGCCGCCGCCACCACGGTGACCTGCACCCGT and TCTAGATTACTGCAGTGGGGC CACT and used to replace the γ CaMKII coding sequence in pCDH-AcGFP- γ CaMKII using NotI and PstI.

Transfection

Cortical neurons were transfected 6–8 days after plating using a high efficiency Ca^{2+} -phosphate transfection method (Jiang and Chen, 2006). HEK293 cells were transfected with Lipofectamine (Life Technologies) according to the manufacturer's instructions.

Lentiviral Transduction of SCG Neurons

To produce lentivirus, the pLVTHM shRNA or pCDH-EF1- γ_A CaMKII constructs were transfected into 293T cells along with the packaging plasmid psPAX2 and the envelope plasmid pMD2.g, kindly provided by Dr. D. Trono (Wiznerowicz and Trono, 2003). After 16 hr, the medium was changed and the supernatant was collected 24 hr later and cleared of cell debris by filtering through a 0.45 μm filter. The viral particles were concentrated by centrifuging the filtrate at $70,000 \times g$ for 2 hr at 4°C using a Beckman SW28 rotor. The viral pellet was then resuspended in sterile PBS, aliquoted, and stored at -80°C . Lentivirus particles (0.5–1 μl of viral stock diluted in 20 μl of PBS per coverslip) were added to SCG cultures containing 500 μl of medium the day after plating. Twenty-four hours later, the cultures were fed with 1 ml of medium and used 2–3 days later, when GFP was detectable in virtually all neurons.

Immunocytochemistry

Cells were fixed in ice-cold 4% paraformaldehyde in phosphate buffer supplemented with 20 mM EGTA and 4% (w/v) sucrose. Fixed cells were then permeabilized with 0.1% Triton X-100, blocked with 6% normal goat serum (or donkey serum) and incubated overnight at 4°C in primary antibodies: goat anti- γ CaMKII (1:500, sc-1541, Santa Cruz); rabbit anti-Ca N (1:500, Cell Signaling Technology); rabbit anti-pCaMKIV (1:500, sc-28443-R, Santa Cruz Biotechnology); mouse anti-CaMKIV (1:500, sc-136249, Santa Cruz Biotechnology); mouse anti-CaM (1:10000, Millipore); rabbit anti-pCREB (1:133, Cell Signaling Technology); goat anti-pCREB (1:500, Santa Cruz); rabbit anti-pCaMKII (1:10000, Cell Signaling Technology); rabbit anti-Ca $\text{v}1.3$ (1:1000, Alomone Labs); mouse anti- β CaMKII (1:1000, Invitrogen); mouse anti- δ CaMKII (1:1000, sc-100362, Santa Cruz); mouse anti-MAP2 antibody (HM-2; 1:1000, Sigma); mouse anti- α CaMKII (1:1000, Invitrogen); mouse anti-HA (1:10000, Convance); mouse anti-HA (1:1000, Sigma-Aldrich); Rabbit anti- β actin (1:100, Cell Signaling Technology). The next day, cells were washed with PBS, incubated at room temperature for 45 min with Alexa secondary antibodies (1:1000, Molecular Probes), washed with PBS and mounted using ProLong Gold (Invitrogen). The cells were imaged with a 60X (1.3 NA) oil objective on an Axioplan epifluorescent microscope equipped with an AxioCam digital camera using AxioVision or confocal microscope LSM 510 (Carl Zeiss, Inc.).

Image Analysis

Images for pCREB quantification were analyzed using a custom-written macro in ImageJ (NIH). The nuclear marker DAPI and an antibody against the neuron-specific protein MAP2 were used to delineate the nucleus and cytoplasm, respectively. A region of interest adjacent to each neuron analyzed was used as an 'off-cell' background. In cortical cultures, α CaMKII was used instead of MAP2 in order to restrict analysis to excitatory neurons. The pCREB level in each neuron was calculated by subtracting the average pCREB channel intensity in the 'off-cell' background region of interest from the average intensity in the nuclear region of interest for each neuron. The nuclear: cytoplasmic ratio was calculated by comparing nuclear immunoreactivity with apical dendrite immunoreactivity (membrane immunoreactivity was not included). To measure the puncta, we captured 8-bit epifluorescent images and subtracted background staining using the rolling ball method (Sternberg, 1983) in ImageJ (National Institutes of Health; see (Mager et al., 2007) for theoretical analysis of a similar approach). After subtraction, we thresholded images such that only those pixels that were 5 units (0–255 scale) above background were counted. A punctum was defined as a region with a minimum of four adjacent suprathreshold pixels. For each punctum, the product of the punctum size and mean pixel intensity (above background) was used as a read-out of the magnitude of the local response or the "punctum weight." The sum of all individual punctum weights per cell was then calculated (also see Wheeler et al., 2012).

Electrophysiology and Field Stimulation

Two platinum electrodes were placed with a distance of ~ 10 mm in the control (5 mM K^+) Tyrode's solution (5K). The cultured SCG neurons on the coverslips were field stimulated at 10 Hz for 60 s with square wave pulses (3 ms per pulse). Amplitude and duration of the pulse was controlled by a Grass S11 stimulator. The stimulus amplitudes were set to 20% above threshold and whole-cell recordings were performed. To reduce any toxicity due to hydrolysis during the field stimulation, the bath solution was perfused at a speed of ~ 0.2 ml/min.

Cytosolic Ca²⁺ Imaging

SCG or cortical neurons were loaded for 30–60 min with 2 μ M Fura-2-AM (Invitrogen) and 0.02% Pluronic F-127 (Invitrogen) in conditioned media in a 37°C/5% CO₂ incubator. Fura-2 fluorescence was probed every 3 s at 37°C by excitation at 340 and 380 nm with a Lambda LS (Sutter Instruments) light source and emission was detected at 510 nm on a Hamamatsu C4742-95 Orca CCD camera (Hamamatsu Photonics). The 340/380 ratio was quantified using regions of interest outlining the entire cell body. Bath solution exchanges were performed via gravity-fed perfusion, with 50% volume exchange in less than 2 s. All solutions contained 0.5 μ M TTX.

Western Blot

SDS-PAGE loading buffer and β -mercaptoethanol were added to the lysate (25 and 10% of the total lysate volume, respectively), and the mixture was heated to 95°C for 5 min. Cellular protein was separated on a 10% SDS-PAGE gel and transferred to Immobilon transfer membrane (Millipore). The membrane was then blocked at room temperature for 1 hr in Odyssey blocking buffer (Li-Cor Biosciences, Lincoln, NE). The membrane was incubated overnight with antibodies such as goat anti- γ CaMKII (1:500, sc-1541, Santa Cruz); rabbit anti-pCaMKII (1:100, Cell Signaling Technology); mouse anti- β CaMKII (1:200, Invitrogen); rabbit anti-Lamin B (1:1000, Cell Signaling Technology); rabbit anti-GAPDH (1:1000, Cell Signaling Technology); rabbit anti- β actin (1:1000, Cell Signaling Technology); mouse anti-HA (1:1000, Sigma). The following day, the membrane was washed with 0.1% Tween 20 in PBS and incubated with an IRDye-labeled secondary antibody (Li-Cor) for 1 hr. After incubation, the membrane was washed with PBS and imaged with Odyssey imaging systems. All the bands were analyzed with Image Studio. For nuclear extraction, the nuclear proteins of cortical neurons (DIV13–15) were isolated with NE-PER Nuclear and Cytoplasmic Extraction Reagent Kit (Thermo Scientific) before the gel electrophoresis.

Immunoprecipitation

Pierce Classic IP Kit (Thermo Fisher) was used to concentrate γ _ACaMKII K43R on agarose beads. Mouse anti-HA antibody (Covance, Munich, Germany) was used to immobilize γ _ACaMKII K43R on the beads and the immunoprecipitated complex was then incubated with or without purified β CaMKII (44 μ g/ml, PV4205, Life Technologies) for 10 s in the presence of 1 mM CaCl₂, 1 μ M CaM, 25 μ M ATP at room temperature. After the incubation, the beads were washed and the immobilized γ _ACaMKII K43R was eluted for Western blot analysis. Rabbit anti-pCaMKII (1:100, Cell Signaling Technology) and goat anti- γ CaMKII (1:50, sc-1541, Santa Cruz) were used to determine the degree of phosphorylation and the total amount of γ _ACaMKII K43R respectively.

Real-Time PCR

Following the indicated stimulation durations, coverslips were placed in RNeasy Lysis Buffer (QIAGEN) and stored at 4°C before use. Total RNA was isolated using an RNeasy Micro kit (QIAGEN) and reverse transcribed into cDNA using a QuantiTect RT-PCR kit (QIAGEN), as per the manufacturer's instructions. Real-time qPCR was performed with SYBR-green PCR master mix (Fermentas) using the DNA engine Opticon 2 (Bio-Rad) through 45 cycles (94°C for 10 s, 60°C for 30 s, 72°C for 30 s). Each cDNA sample, equivalent to RNA from one 10 mM coverslip of cultured cells, was run in duplicate for the target gene (*c-fos* or *γ CaMKII*) and the housekeeping genes (*β -actin*, *PPP1ca*, and *GAPDH* or *EGFP*). In each experiment, 3 separate coverslips were used per condition. Specificity of amplicons was determined by melting-curve analysis, gel electrophoresis, and DNA sequencing. The ratio of fold-change in expression of the mRNA of interest for each sample was calculated by normalization of cycle threshold (Ct) values of the target gene to each of the housekeeping genes using the comparative $\Delta\Delta C(t)$ method. Data are reported as the average ratio of fold change in mRNA of interest corrected for reference gene ($2^{-\Delta\Delta C(t)}$). Data were analyzed using one-way ANOVAs with Student-Newman-Keuls Multiple Comparisons posthoc tests (p values). Primer pair sequences (forward/reverse) were as follows: *c-fos* 5'-ATC GGC AGA AGG GGC AAA GTA G-3'/5'-GCA ACG CAG ACT TCT CGT CTT CA AG-3'; *γ CaMKII* 5'-AAG AAG TTG TCT GCC CGA GA-3'/5'-CCT CCC GTA ACA AGG TCA AA-3'; *β -actin* 5'-AGG CCC CTC TGA ACC CTA AG-3'/5'-CCA GAG GCA TAC AGG GAC AAC-3'; *Ppp1ca* 5'-ATG AGT GTG CCA GCA TCA AC-3'/5'-CAG TTG AAG CAG TCG GTG AA-3'; *GAPDH* 5'-AAC CTGC CAA GTA TGA TGA CAT CA-3'/5'-TGT TGA AGT CAC AGG AGA CAA CCT-3'; *EGFP* 5'-GAC GAC GGC AAC TAC AAG A-3'/5'-GAT GCC GTT CTT CTG CTT-3'. All primers were synthesized by Eurofins MWG Operon.

Sample Preparation and Mass Spectrometry Analysis

HA-tagged γ _ACaMKII plasmids were transfected into HEK293 cells. 48 hr after transfection, the cells were washed with ice-cold PBS and lysed with IP Lysis buffer (Thermo Fisher) containing a protease inhibitor cocktail tablet (Roche, Indianapolis, IN). Lysates were incubated with anti-HA antibody (Covance, Munich, Germany) and Protein A sepharose beads. The immunoprecipitated complex was then incubated with purified CaN and reaction buffer containing CaM (Enzo Life Sciences) and separated by SDS-PAGE. Corresponding areas showing γ _ACaMKII-IR on immunoblots were cut out from the Coomassie blue-stained SDS-PAGE gels. Gel pieces underwent in-gel digestion according to (Shevchenko et al., 1996) and the phosphopeptides were enriched by titanium dioxide (GL Sciences Inc., Japan) based on a previously published protocol (Rappsilber et al., 2007). Resulting peptides were subjected to nano-LC-MS/MS analysis using a Thermo Scientific EASY-nLC 1000 coupled to a Q Exactive mass spectrometer (Thermo Fisher Scientific). A self packed 75 μ m \times 25 cm reversed phase column (Reprosil C18, 3 μ m, Dr. Maisch GmbH, Germany) was used for peptide separation. Peptides were eluted by a gradient of 3%–30% acetonitrile in 0.1% formic acid over 60 min at a flow rate of 250 nL/min. The Q Exactive was operated in the data-dependent mode with survey scans acquired at a resolution of 50,000 at m/z 400. Up to the

top 10 most abundant precursors from the survey scan were selected with an isolation window of 1.6 Thomsons and fragmented by higher energy collisional dissociation with normalized collision energies of 27. The maximum ion injection times for the survey scan and the MS/MS scans were 20 and 60 ms, respectively, and the ion target value for both scan modes were set to 1,000,000. Each sample was processed and analyzed in triplicate.

Phosphopeptide Identification and Quantitation

The raw files were processed using the MaxQuant (Cox and Mann, 2008) computational proteomics platform version 1.2.7.0 for peptide identification and quantitation. The fragmentation spectra were searched against the Uniprot rat protein database allowing up to two missed tryptic cleavages. Carbamidomethylation of cysteine was set as a fixed modification, and phosphorylation of serine/threonine/tyrosine, oxidation of methionine and protein N-terminal acetylation were used as variable modifications for database searching. The precursor and fragment mass tolerances were set to 7 and 20 ppm, respectively. Quantitation of the phosphopeptide RKS (Phospho) SSSVHLM (oxidation) EPQTTVVHNATDGIK was performed using the ion intensity values calculated by MaxQuant for the quintuply charged peptide ion with an m/z value of 564.4773. Normalization of phosphopeptide intensities to global peptide intensities had no effect on calculated ratios.

SUPPLEMENTAL REFERENCES

- Cohen, P., Holmes, C.F., and Tsukitani, Y. (1990). Okadaic acid: a new probe for the study of cellular regulation. *Trends Biochem. Sci.* 15, 98–102.
- Cox, J., and Mann, M. (2008). MaxQuant enables high peptide identification rates, individualized p.p.b.-range mass accuracies and proteome-wide protein quantification. *Nat. Biotechnol.* 26, 1367–1372.
- Enslen, H., Tokumitsu, H., Stork, P.J., Davis, R.J., and Soderling, T.R. (1996). Regulation of mitogen-activated protein kinases by a calcium/calmodulin-dependent protein kinase cascade. *Proc. Natl. Acad. Sci. USA* 93, 10803–10808.
- Ferreira, M.A., O'Donovan, M.C., Meng, Y.A., Jones, I.R., Ruderfer, D.M., Jones, L., Fan, J., Kirov, G., Perlis, R.H., Green, E.K., et al.; Wellcome Trust Case Control Consortium (2008). Collaborative genome-wide association analysis supports a role for ANK3 and CACNA1C in bipolar disorder. *Nat. Genet.* 40, 1056–1058.
- Gerber, D.J., Hall, D., Miyakawa, T., Demars, S., Gogos, J.A., Karayiorgou, M., and Tonegawa, S. (2003). Evidence for association of schizophrenia with genetic variation in the 8p21.3 gene, PPP3CC, encoding the calcineurin gamma subunit. *Proc. Natl. Acad. Sci. USA* 100, 8993–8998.
- Hawrot, E., and Patterson, P.H. (1979). Long-term culture of dissociated sympathetic neurons. *Methods Enzymol.* 58, 574–584.
- Jiang, M., and Chen, G. (2006). High Ca²⁺-phosphate transfection efficiency in low-density neuronal cultures. *Nat. Protoc.* 1, 695–700.
- Kim, S.H., Yu, H.S., Park, H.G., Ha, K., Kim, Y.S., Shin, S.Y., and Ahn, Y.M. (2013). Intracerebroventricular administration of ouabain, a Na/K-ATPase inhibitor, activates mTOR signal pathways and protein translation in the rat frontal cortex. *Prog. Neuropsychopharmacol. Biol. Psychiatry* 45, 73–82.
- Liu, Y.L., Fann, C.S., Liu, C.M., Chang, C.C., Yang, W.C., Hung, S.I., Yu, S.L., Hwang, T.J., Hsieh, M.H., Liu, C.C., et al. (2007). More evidence supports the association of PPP3CC with schizophrenia. *Mol. Psychiatry* 12, 966–974.
- Mager, D.E., Kobrinsky, E., Masoudieh, A., Maltsev, A., Abernethy, D.R., and Soldatov, N.M. (2007). Analysis of functional signaling domains from fluorescence imaging and the two-dimensional continuous wavelet transform. *Biophys. J.* 93, 2900–2910.
- Mathieu, F., Miot, S., Etain, B., El Khoury, M.A., Chevalier, F., Bellivier, F., Leboyer, M., Giros, B., and Tzavara, E.T. (2008). Association between the PPP3CC gene, coding for the calcineurin gamma catalytic subunit, and bipolar disorder. *Behav. Brain Funct.* 4, 2.
- Miyakawa, T., Leiter, L.M., Gerber, D.J., Gainetdinov, R.R., Sotnikova, T.D., Zeng, H., Caron, M.G., and Tonegawa, S. (2003). Conditional calcineurin knockout mice exhibit multiple abnormal behaviors related to schizophrenia. *Proc. Natl. Acad. Sci. USA* 100, 8987–8992.
- Nagao, M., Shima, H., Nakayasu, M., and Sugimura, T. (1995). Protein serine/threonine phosphatases as binding proteins for okadaic acid. *Mutat. Res.* 333, 173–179.
- Novak, G., Seeman, P., and Talerico, T. (2000). Schizophrenia: elevated mRNA for calcium-calmodulin-dependent protein kinase IIbeta in frontal cortex. *Brain Res. Mol. Brain Res.* 82, 95–100.
- Nyegaard, M., Demontis, D., Foldager, L., Hedemand, A., Flint, T.J., Sørensen, K.M., Andersen, P.S., Nordentoft, M., Werge, T., Pedersen, C.B., et al. (2010). CACNA1C (rs1006737) is associated with schizophrenia. *Mol. Psychiatry* 15, 119–121.
- Rappsilber, J., Mann, M., and Ishihama, Y. (2007). Protocol for micro-purification, enrichment, pre-fractionation and storage of peptides for proteomics using StageTips. *Nat. Protoc.* 2, 1896–1906.
- Shevchenko, A., Wilm, M., Vorm, O., and Mann, M. (1996). Mass spectrometric sequencing of proteins silver-stained polyacrylamide gels. *Anal. Chem.* 68, 850–858.
- Sklar, P.; Psychiatric GWAS Consortium Bipolar Disorder Working Group (2011). Large-scale genome-wide association analysis of bipolar disorder identifies a new susceptibility locus near ODZ4. *Nat. Genet.* 43, 977–983.
- Sklar, P., Smoller, J.W., Fan, J., Ferreira, M.A., Perlis, R.H., Chambert, K., Nimgaonkar, V.L., McQueen, M.B., Faraone, S.V., Kirby, A., et al. (2008). Whole-genome association study of bipolar disorder. *Mol. Psychiatry* 13, 558–569.
- Splawski, I., Timothy, K.W., Sharpe, L.M., Decher, N., Kumar, P., Bloise, R., Napolitano, C., Schwartz, P.J., Joseph, R.M., Condouris, K., et al. (2004). Ca(V)1.2 calcium channel dysfunction causes a multisystem disorder including arrhythmia and autism. *Cell* 119, 19–31.
- Splawski, I., Timothy, K.W., Decher, N., Kumar, P., Sachse, F.B., Beggs, A.H., Sanguinetti, M.C., and Keating, M.T. (2005). Severe arrhythmia disorder caused by cardiac L-type calcium channel mutations. *Proc. Natl. Acad. Sci. USA* 102, 8089–8096, discussion 8086–8088.
- Sternberg, S.R. (1983). Biomedical Image-Processing. *Computer* 16, 22–34.
- Sullivan, P.F., de Geus, E.J., Willemsen, G., James, M.R., Smit, J.H., Zandbelt, T., Arolt, V., Baune, B.T., Blackwood, D., Cichon, S., et al. (2009). Genome-wide association for major depressive disorder: a possible role for the presynaptic protein piccolo. *Mol. Psychiatry* 14, 359–375.

- Sumi, M., Kiuchi, K., Ishikawa, T., Ishii, A., Hagiwara, M., Nagatsu, T., and Hidaka, H. (1991). The newly synthesized selective Ca²⁺/calmodulin dependent protein kinase II inhibitor KN-93 reduces dopamine contents in PC12h cells. *Biochem. Biophys. Res. Commun.* 181, 968–975.
- Wiznerowicz, M., and Trono, D. (2003). Conditional suppression of cellular genes: lentivirus vector-mediated drug-inducible RNA interference. *J. Virol.* 77, 8957–8961.
- Yu, J.J., Zhang, Y., Wang, Y., Wen, Z.Y., Liu, X.H., Qin, J., and Yang, J.L. (2013). Inhibition of calcineurin in the prefrontal cortex induced depressive-like behavior through mTOR signaling pathway. *Psychopharmacology (Berl.)* 225, 361–372.
- Zhu, W.L., Shi, H.S., Wang, S.J., Wu, P., Ding, Z.B., and Lu, L. (2011). Hippocampal CA3 calcineurin activity participates in depressive-like behavior in rats. *J. Neurochem.* 117, 1075–1086.

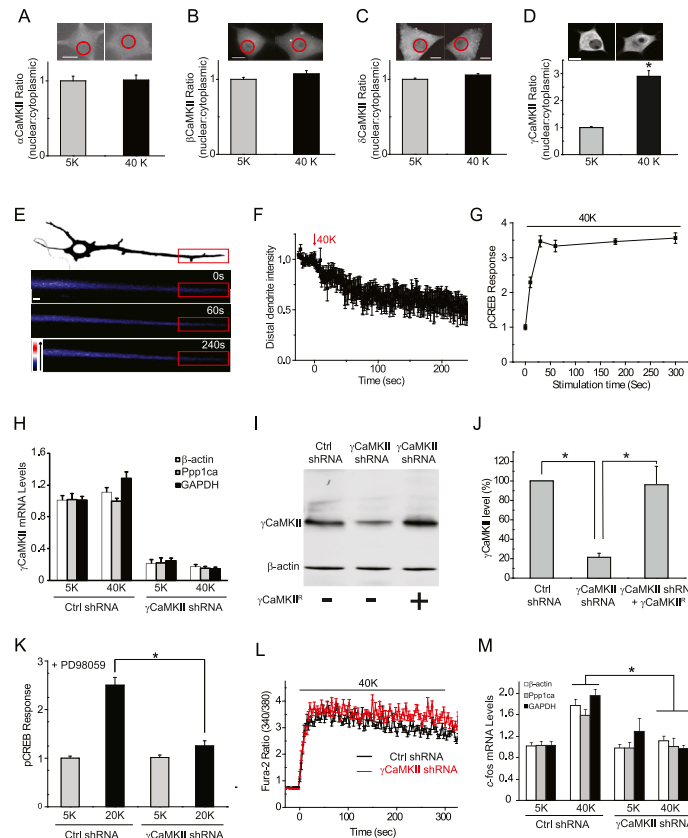


Figure S1. Examine the Distribution of CaMKII Isoforms and pCREB Response in SCG Neurons, Related to Figure 1

(A–C) SCG neurons were either mock-stimulated in 5 mM K^+ Tyrode solution (containing 2 mM Ca^{2+}) or stimulated with 40 mM K^+ Tyrode solution for 300 s. After stimulation, cells were immediately fixed in 4% paraformaldehyde and stained for α CaMKII (A), β CaMKII (B), or δ CaMKII (C). Scale bar, 10 μ m. There is no significant change in nuclear: cytoplasmic ratio for α CaMKII, β CaMKII, or δ CaMKII following stimulation.

(D) Representative confocal images of the γ CaMKII in SCG neurons after 40 mM K^+ stimulation for 300 s compared with 5 mM K^+ mock-stimulation. Scale bar, 10 μ m. The nuclear: cytoplasmic ratio of γ CaMKII intensity increase significantly following stimulation. Quantification was based on ≥ 16 fields ($n \geq 20$ cells) under a 40 \times objective from 2 platings per condition.

(E) The intensity of mGFP- γ CaMKII in the distal dendrite was measured upon 40 mM K^+ stimulation. The ROI used for the measurement is marked in a red box in the schematic SCG neuron (upper row). The other panels show epifluorescence images captured at time points 0 s, 60 s, and 240 s after onset of stimulation. The GFP signal is presented in the union jack format, with color changing from dark blue to white to red as intensity increases. Scale bar, 2 μ m.

(F) Time-lapse imaging revealed that γ CaMKII in distal dendrites decreased progressively following 40 mM K^+ stimulation ($n = 7$).

(G) SCG neurons were stimulated with 40 mM K^+ for different durations, immediately fixed, and pCREB response was measured. The pCREB response rose rapidly and reached maximum after 40 mM K^+ stimulation for 30 s.

(H) γ CaMKII shRNA was packaged into lentivirus and overexpressed in SCG neurons. Compared to nonsilencing control shRNA, γ CaMKII shRNA reduced γ CaMKII mRNA levels by $\sim 80\%$ in SCG neurons. GAPDH, Ppp1ca and β -actin were used as internal references for RT-PCR. The shRNA against γ CaMKII had no detectable effect on mRNA levels of the other isoforms of CaMKII (data not shown).

(I and J) Western blot to examine γ CaMKII protein levels in SCG neurons following shRNA knockdown. In SCG neurons transduced with γ CaMKII shRNA, γ CaMKII protein levels were only $\sim 20\%$ of that found in nonsilencing control shRNA-transduced neurons; right lane and bar demonstrate rescue by overexpressed γ CaMKII shRNA resistant γ CaMKII^R. Quantification based on 7 platings per condition.

(K) Lentiviral-transduced SCG neurons expressing γ CaMKII shRNA or nonsilencing control shRNA were stimulated with 20 mM K^+ for 300 s (using 20 mM K^+ instead of 40 mM K^+ to avoid saturating pCREB response) in the presence of PD98059 (50 μ M), a specific inhibitor for Ras/mitogen-activated protein kinase kinase (MEK). This was a precaution against the possibility that γ CaMKII knockdown might exert indirect effects on MAPK signaling to CREB phosphorylation, via CaMKIV (Enslen et al., 1996; Wu et al., 2001). γ CaMKII knockdown prevented the pCREB response. Quantification was based on ≥ 24 fields ($n \geq 30$ cells) under a 63 \times objective from 3–6 platings per condition.

(L) SCG neurons transduced as in (K) were stimulated with 40 mM K^+ for 300 s. The calcium transient upon stimulation was assessed by monitoring the Fura-2 emission ratio (340/380). No difference in amplitude or time course of the rise in cytoplasmic Ca^{2+} ($n \geq 20$). (M) *c-fos* mRNA levels in SCG neurons transduced as in (K) and stimulated with 40 mM K^+ for 300 s, followed by 40 min incubation in normal culture medium to allow time for novel transcription. γ CaMKII knockdown prevented transcription of *c-fos*. Data are normalized against three housekeeping genes and normalized to *c-fos* levels in the control stimulation condition with nonsilencing control shRNA. For RT-PCR, $N = 3$ –4 experiments done in triplicate. * $p < 0.001$ as determined by Student's *t* test. Data are represented as mean \pm SEM.

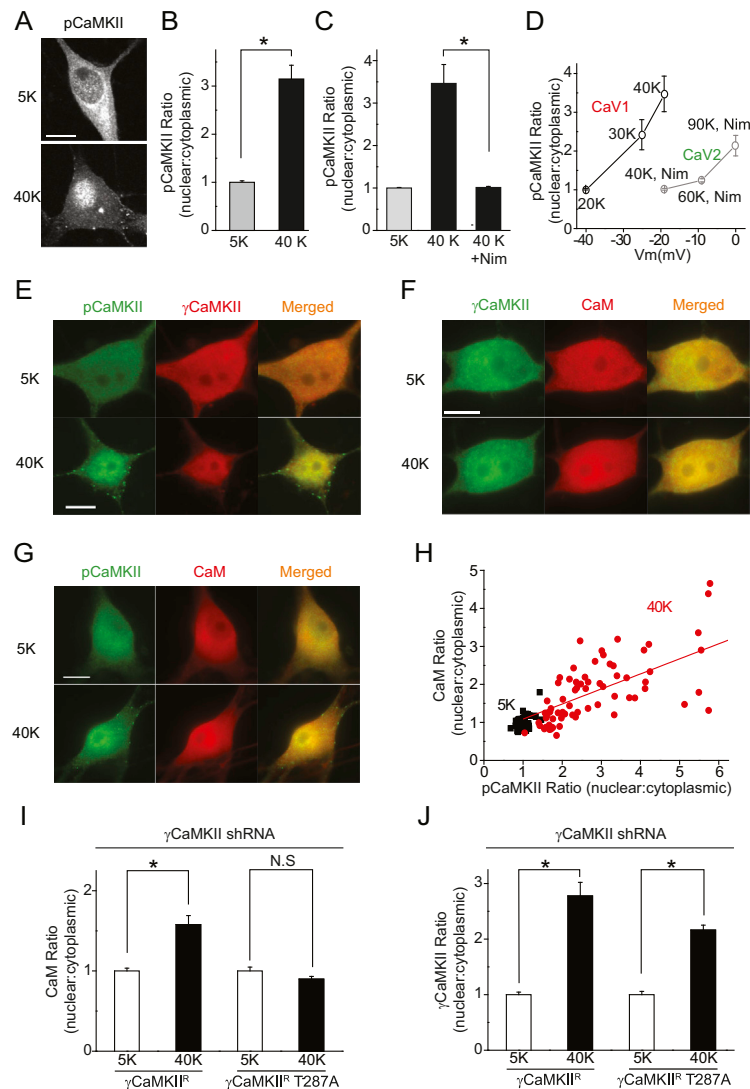


Figure S2. Activity-Dependent pCaMKII Redistribution and γ CaMKII/CaM Translocation, Related to Figure 2

(A and B) SCG neurons were mock-stimulated with 5 mM K⁺ or stimulated with 40 mM K⁺ and stained for pCaMKII (Thr286/287). Representative confocal images (A) show a significant change of pCaMKII distribution (B). Quantification was based on ≥ 16 fields ($n \geq 20$ cells) under a 40x objective from 2 platings per condition.

(C) pCaMKII redistribution triggered by 40 mM K⁺ stimulation was abolished by applying the Ca_v1 specific blocker Nim (10 μM).

(D) With calcium influx from Ca_v1 and Ca_v2 channels distinguished by the Ca_v1 specific blocker Nim (10 μM), pCaMKII distribution ratio was plotted against the depolarized membrane potential level (membrane potential data from Wheeler et al., 2012). Compared to Ca_v2 signaling (gray line), calcium influx through Ca_v1 channels (black line) was more potent in changing the pCaMKII distribution.

(E) SCG neurons treated as in (A) were co-stained with antibodies against pCaMKII and γ CaMKII. Representative images show nuclear translocation of γ CaMKII is accompanied by pCaMKII redistribution.

(F) SCG neurons treated as in (A) were co-stained with antibodies against γ CaMKII and CaM. Representative images show nuclear translocation of γ CaMKII is accompanied by CaM translocation.

(G) SCG neurons treated as in (A) were co-stained with antibodies against pCaMKII and CaM. Representative images show nuclear translocation of pCaMKII is accompanied by CaM redistribution.

(H) Single-cell correlation of nuclear: cytoplasmic intensity ratio between CaM and pCaMKII, in response to 40 mM K⁺ stimulation for 300 s. The red solid line is a linear fit of the data ($R = 0.8$).

(I and J) Lentiviral transduced SCG neurons expressing γ CaMKII shRNA with γ CaMKII shRNA resistant γ CaMKII^R or γ CaMKII^R 287A were stimulated with 40 mM K⁺ for 300 s and co-stained for γ CaMKII and CaM. CaM translocation was rescued by shRNA resistant γ CaMKII^R but not by γ CaMKII^R 287A (I), even though both γ CaMKII^R and γ CaMKII^R 287A can translocate to the nucleus upon the stimulation (J). Scale bar, 10 μm. * $p < 0.001$ as determined by Student's t test. Data are represented as mean \pm SEM.

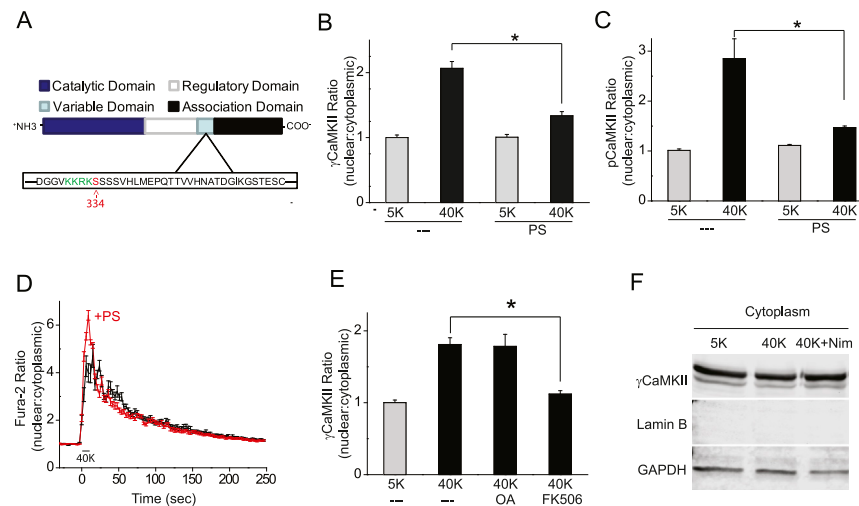


Figure S3. CaN Activity Is Critical for γ CaMKII Translocation in SCG and Cortical Neurons, Related to Figure 3

(A) The organization of functional domains of the CaMKII protein. γ_A CaMKII has a nuclear localization signal (KKRK) in the variable domain, followed by four serines.

(B and C) SCG neurons were stimulated with 40 mM K^+ for 300 s in the absence or presence of the broad spectrum phosphatase inhibitor PhosStop (PS, 1 tablet in 10 ml Tyrode solution). The γ CaMKII translocation (B) and nuclear pCaMKII increase (C) were both inhibited by applying PS.

(D) Calcium transients (Fura-2, 340/380 ratio) were measured when SCG neurons were stimulated with 40 mM K^+ for 10 s in the absence or presence of the broad phosphatase inhibitor PhosStop (PS, 1 tablet in 10 ml Tyrode solution). After stimulation, SCG neurons were rinsed with 5 K^+ Tyrode solution.

(E) SCG neurons were stimulated as in (B), in the absence or presence of OA (2 μM , sufficient to block both PP2A and PP1) (Cohen et al., 1990; Nagao et al., 1995) or CaN inhibitor FK506 (1 μM). After stimulation, neurons were stained for γ CaMKII. FK506 but not OA prevented γ CaMKII translocation.

(F) Cytoplasm was isolated from cultured cortical neurons (Thermo Scientific) and Western blot analysis was performed to probe for γ CaMKII. 40 mM K^+ stimulation of intact cells induced what appeared to be a $\sim 10\%$ decrease in cytosolic levels of γ CaMKII ($p = 0.23$), which seemed to be prevented by the Ca_v1 blocker Nim ($p = 0.56$) ($n = 4$). Lamin B is a nuclear marker to assess the purity of the isolated cytoplasm and GAPDH is a loading control. * $p < 0.001$, as determined by student's t test. Data are represented as mean \pm SEM.

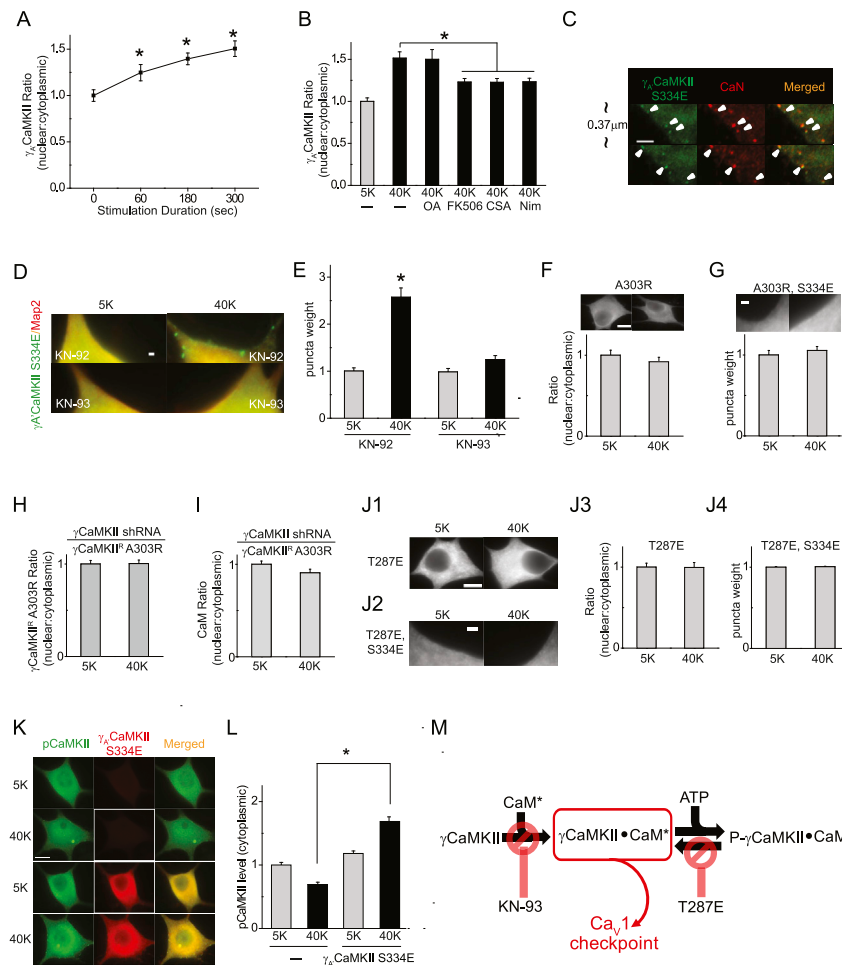


Figure S4. γ CaMKII Is Recruited to a Signaling Checkpoint in a CaM-Bound, but Not a Thr287-Phosphorylated, Form, Related to Figure 4

(A) Lentiviral-transduced SCG neurons expressing HA-tagged γ _ACaMKII were stimulated with 40 mM K⁺ for different durations. The maximum translocation of γ _ACaMKII was observed with a stimulation for 300 s.

(B) Lentiviral transduced SCG neurons expressing HA-tagged γ _ACaMKII were stimulated with 40 mM K⁺ for 300 s in the presence or absence of OA (2 μ M), FK506 (1 μ M), CsA (50 nM) or Nim (10 μ M). As in the case of endogenous γ CaMKII, the translocation of overexpressed γ _ACaMKII was prevented by the CaN inhibitors FK506 or CsA, the Ca_v1 blocker Nim, but not by OA.

(C) Lentiviral transduced SCG neurons expressing HA-tagged γ _ACaMKII S334E were stimulated with 40 mM K⁺ for 60 s and stained with antibodies against the HA tag on γ _ACaMKII S334E and against CaN. Arrows indicate sites at which γ _ACaMKII S334E puncta colocalize with CaN. In the upper row, the focal plane was shifted upward along the z-axis by ~0.37 μ m, away from the coverslip, yet colocalized puncta could nevertheless be observed. Scale bar, 5 μ m.

(D) To test whether γ _ACaMKII must bind CaM before it is mobilized to the surface checkpoint, we overexpressed γ _ACaMKII S334E and stimulated SCG neurons with 40 mM K⁺ in the presence of KN-93 (4 μ M), an agent that interferes with CaMKII-CaM interactions (Sumi et al., 1991), or KN-92 its inactive congener. Representative images; Scale bar, 1 μ m.

(E) γ _ACaMKII S334E puncta weight was calculated as described in Methods. KN-93 prevented γ _ACaMKII S334E puncta formation at the cell surface whereas KN-92 did not.

(F and G) Representative images of SCG neurons overexpressing γ _ACaMKII A303R (deficient in CaM binding) or γ _ACaMKII A303R, S334E upon 40 mM K⁺ stimulation. Scale bar is 10 μ m for (F) and 5 μ m for (G). γ _ACaMKII A303R does not translocate to the nucleus upon 40 mM K⁺ stimulation (F). Unlike γ _ACaMKII, γ _ACaMKII A303R, S334E does not form puncta on the cell surface upon the stimulation (G).

(H and I) With endogenous γ CaMKII knocked down, γ _ACaMKII^R A303R failed to translocate to the nucleus (H) or to rescue CaM translocation (I).

(J1–J4) Representative images of SCG neurons overexpressing γ _ACaMKII T287E (mimicking the phosphorylation at Thr287) or γ _ACaMKII T287E, S334E upon 40 mM K⁺ stimulation. Scale bar is 10 μ m for (J1) and 5 μ m for (J2). γ _ACaMKII T287E does not translocate to the nucleus upon 40 mM K⁺ stimulation (J3). Unlike γ _ACaMKII S334E, γ _ACaMKII T287E S334E does not form puncta on the cell surface upon the stimulation (J4).

(K and L) pCaMKII levels in the cytoplasm after stimulation. Following γ _ACaMKII S334E overexpression, cytosolic pCaMKII levels increased significantly upon stimulation.

(M) Schematic figure indicating that, in order to translocate to the nucleus, γ _ACaMKII must bind CaM in a dephosphorylated (Thr287) state to be recruited to a checkpoint where CaN is localized. *p < 0.001 as determined by Student's t test. Data are represented as mean \pm SEM.

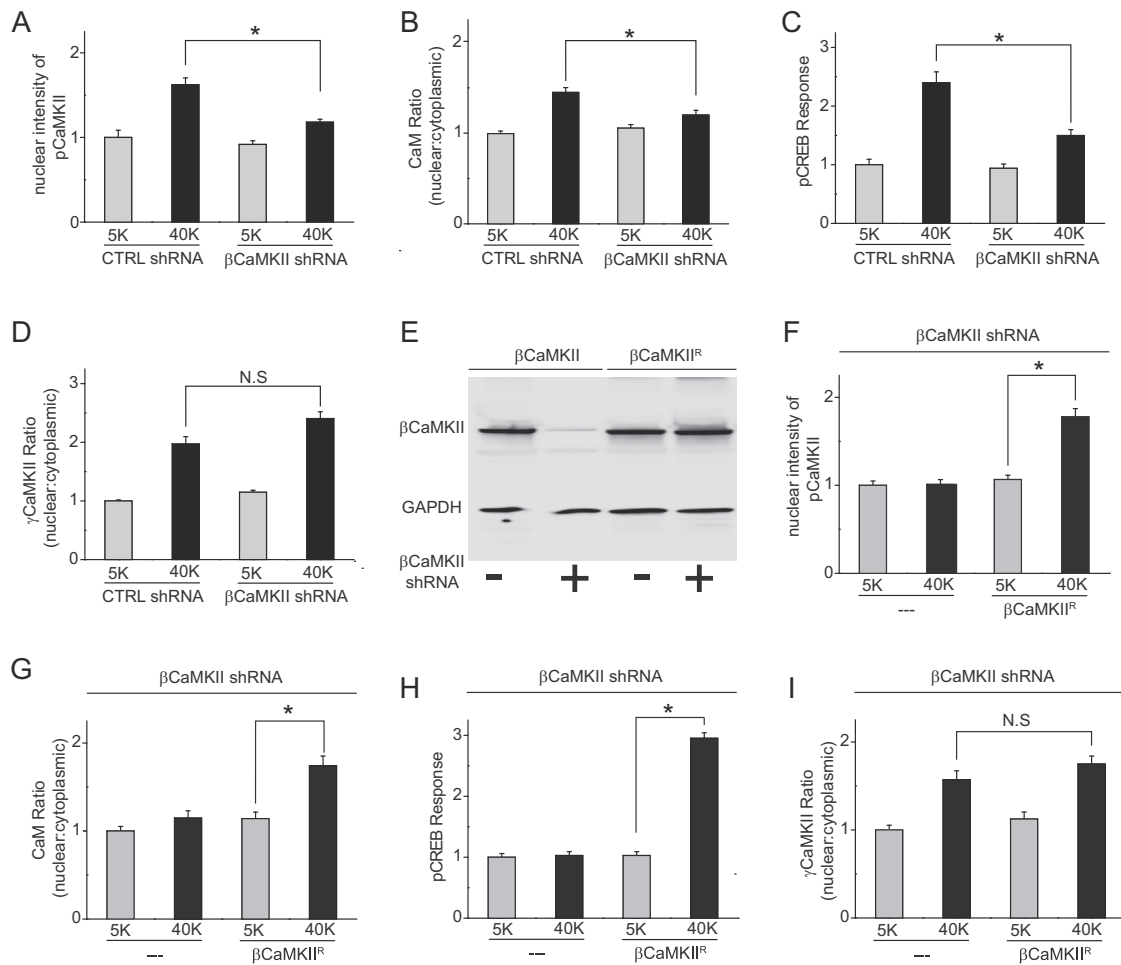


Figure S5. βCaMKII Is Dispensable for γCaMKII Translocation but Is Required for pCaMKII Redistribution, CaM Translocation, and CREB Phosphorylation, Related to Figure 5

(A–D) Lentiviral-transduced SCG neurons expressing βCaMKII shRNA or nonsilencing control shRNA were stimulated with 40 mM K⁺ for 300 s and stained for pCaMKII, co-stained for γCaMKII and CaM, or stained for pCREB. βCaMKII knock-down prevented the increase in nuclear pCaMKII levels (A), CaM translocation (B) and pCREB response (C), but did not affect γCaMKII translocation (D).

(E) mGFP-tagged βCaMKII or βCaMKII shRNA-resistant mGFP-βCaMKII^R was overexpressed in HEK293 cells with or without the presence of βCaMKII shRNA. In the presence of βCaMKII shRNA, only ~3% of basal βCaMKII was expressed (left two lanes, $p < 0.001$, $n = 4$), while βCaMKII shRNA spared the expression of βCaMKII^R (right two lanes, $p > 0.5$, $n = 4$). GAPDH was used as a loading control.

(F–I) Lentiviral-transduced SCG neurons expressing βCaMKII shRNA with βCaMKII shRNA resistant βCaMKII^R were stimulated with 40 mM K⁺ for 300 s (F, G, H) or 10 s (I) and stained for pCaMKII, CaM, pCREB or γCaMKII. Nuclear increase of pCaMKII (F), CaM translocation (G), and pCREB response (H) were effectively rescued by shRNA-resistant βCaMKII^R, while γCaMKII translocation was not affected (I). * $p < 0.001$ as determined by Student's *t* test. All the intensity ratios were normalized to the ratio with 5 mM K⁺ mock-stimulation in control neurons. Quantification was based on ≥ 24 fields ($n \geq 30$ cells) under a 63x objective from 3–6 platings per condition. Data are represented as mean \pm SEM.

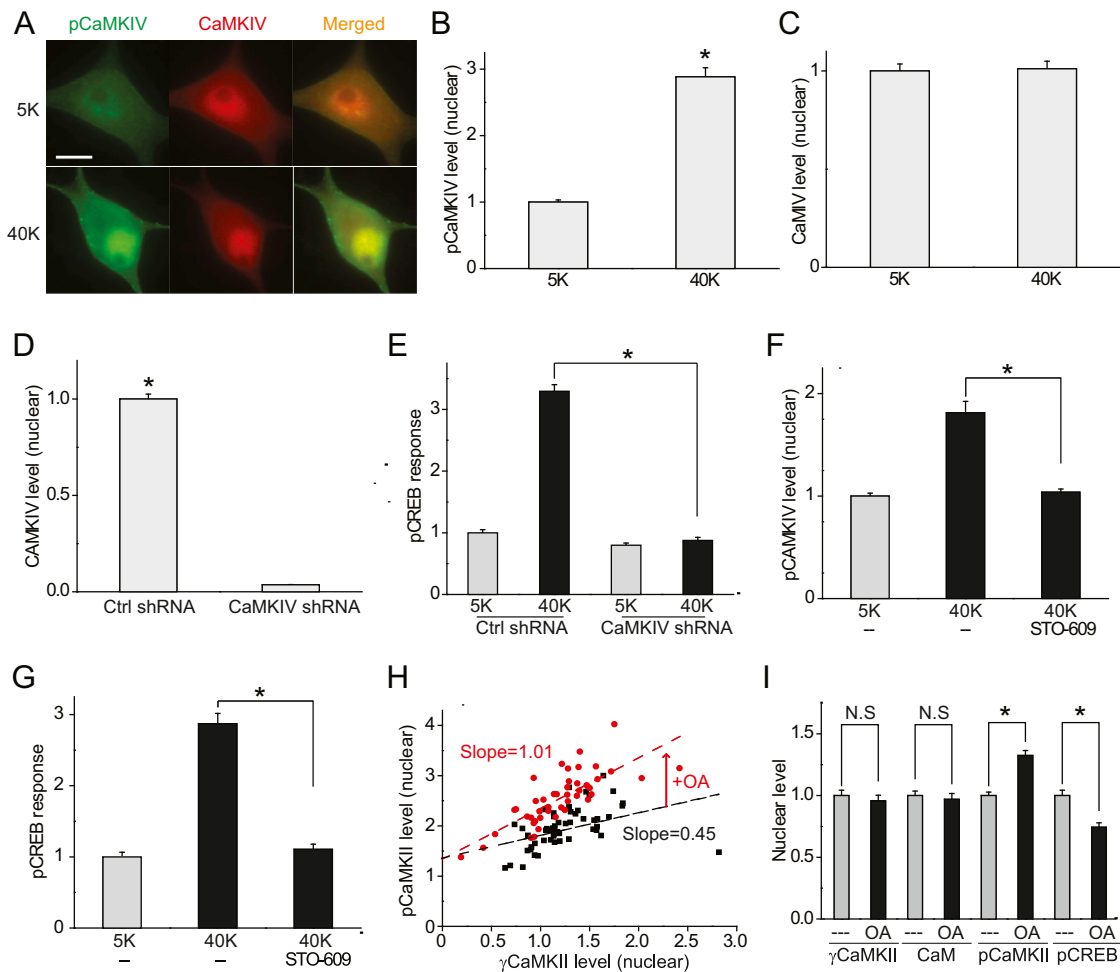


Figure S6. Free CaM Drives Activation of a CaM Kinase Cascade within the Nucleus, Related to Figure 6

(A) Representative images for SCG neurons stimulated with 40 mM K^+ for 300 s and stained for pCaMKIV (phospho-Thr196) and CaMKIV. Scale bar, 10 μ m.

(B and C) SCG neurons were treated as in (A), and the nuclear levels of pCaMKIV (B) and CaMKIV (C) were measured. While nuclear pCaMKIV levels increased significantly upon stimulation (B), no significant change in the level of nuclear CaMKIV was observed (C).

(D) Lentiviral transduced SCG neurons expressing CaMKIV shRNA or nonsilencing control shRNA were stained with anti-CaMKIV antibody. After CaMKIV knockdown, less than 1% CaMKIV immunoreactivity remained in the nucleus.

(E) Lentiviral transduced SCG neurons expressing CaMKIV shRNA or nonsilencing control shRNA were stimulated with 40 mM K^+ for 10 s and stained for pCREB. CaMKIV knockdown prevented the pCREB response in the nucleus.

(F and G) SCG neurons were stimulated with 40 mM K^+ for 10 s in the absence and presence of 3 μ M STO-609, a specific inhibitor for CaMKK. Increases in nuclear pCaMKIV (F) and pCREB (G) response were abolished in the presence of the CaMKK inhibitor.

(H) Testing for involvement of PP2A in dephosphorylation of nuclear pCaMKII. SCG neurons were stimulated with 40 mM K^+ in the absence or presence of 20 nM okadaic acid (OA) to specifically inhibit PP2A. Nuclear pCaMKII level after stimulation was plotted against the nuclear γ CaMKII level. Linear regression lines were compared between the groups with (red) and without OA (black). The slope for the OA group is more than two-fold steeper than for the group without OA, indicating that more γ CaMKII was in a Thr287 phosphorylated form after nuclear import with PP2A inhibited by OA.

(I) Comparison of nuclear pCaMKII and γ CaMKII values from (H). OA increased significantly the nuclear pCaMKII level after stimulation, without changing the γ CaMKII and CaM level; notably, nuclear CREB phosphorylation was significantly diminished. These data are consistent with a scenario in which PP2A serves to dephosphorylate T287-phosphorylated γ CaMKII, thus liberating trapped CaM and driving the nuclear CaM cascade; OA would oppose such an action. * $p < 0.001$, as determined by Student's *t* test. Data are represented as mean \pm SEM.

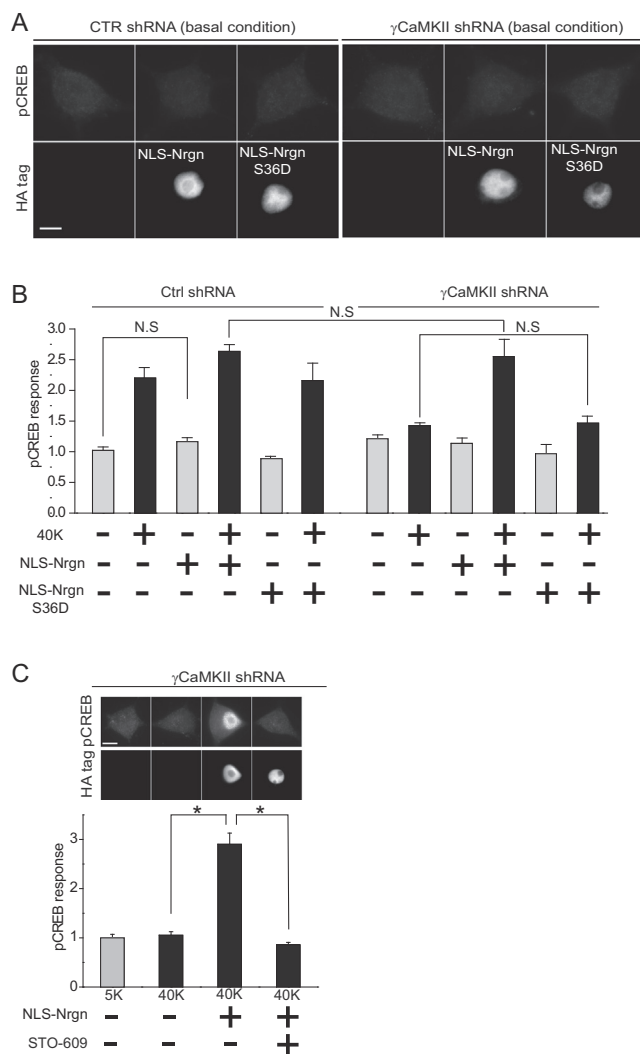


Figure S7. CaM Is Sufficient for Triggering CREB Phosphorylation, Related to Figure 7

(A and B) Lentiviral transduced SCG neurons expressing γ CaMKII shRNA or nonsilencing control shRNA were stimulated with 40 mM K^+ for 10 s. NLS-Nrgn (but not NLS-Nrgn S36D) was able to restore the pCREB response, consistent, respectively, with its ability (or inability) to release free CaM upon the rise in nuclear Ca^{2+} . Under basal conditions, overexpressing NLS-Nrgn or NLS-Nrgn S36D does not affect pCREB levels. Scale bar, 10 μ m. N.S. connotes $p > 0.05$ as determined by Student's t test. Quantification was based on ≥ 24 fields ($n \geq 30$ cells) under a 63 \times objective from 3 platings per condition. Error bars represent SEM.

(C) Lentiviral transduced SCG neurons expressing γ CaMKII shRNA were stimulated with 40 mM K^+ for 10 s. NLS-Nrgn restored the pCREB response and the restoration was prevented by specific CaMKK inhibitor STO-609, consistent with the idea that CaM delivery operates upstream of the activation of nuclear CaMKK-CaMKIV-pCREB cascade.